5

Mobile Velocity Estimation for Wireless Communications

Bouchra Senadji
Queensland University of Technology

Ghazem Azemi
Queensland University of Technology

Boualem Boashash
Queensland University of Technology

Abstract

In this chapter we explain the principles of velocity estimation and review both analytically and using simulations the properties of existing estimators. We then discuss the importance of accurate velocity estimation in the context of handover algorithm design. We show how an error in velocity estimation can significantly increase the probability of dropped calls, leading to a poorer quality of service of the system. Some velocity estimators require prior estimation of the Rician factor. This chapter also presents two Rice factor estimators that have been shown to have better performance than existing estimators.

5.1 Introduction

This chapter presents the principles of mobile velocity estimation and illustrates its importance in the context of handoff algorithm design for mobile communications systems. Current mobile communications systems are under constant pressure to increase their capacity while maintaining a high quality of service. This is due to an ever-growing population of mobile phone users and an increasing demand for multimedia services. The main constraints system designers have to face are the distortions introduced by the mobile communications channel. These can be classified as Rayleigh or Rician fading, shadowing, and path loss [62, p. 16].[1] These distortions limit the performance of mobile communications systems in terms of efficiency and quality of service. Many standard functions of the system are significantly enhanced by *a priori* knowledge or estimation of the *mobile velocity*. The next section provides examples where mobile velocity plays a key role in the overall performance of the communications system.

5.1.1 Importance of Velocity Estimation

In microcellular systems, the cell size is smaller than in macrocellular systems (Figure 5.1). As a result, microcellular systems require faster and more reliable handovers.[2] Also, since the base station (BS) is at lamppost level, if the mobile station (MS) rounds a corner, the signal power received by an MS can drop rapidly by 20 to 30 dB over distances as small as 10 m (Figure 5.2 and Figure 5.3) [6]. In that case, an emergency handover needs to be processed toward a target BS if the call is to be maintained. The drop in signal strength can be detected by applying short temporal window averaging in the received signal. However, the window size is velocity dependent and is optimal only when an accurate estimation of the mobile velocity is available [7].

In multitier systems (Figure 5.1), cells of different sizes coexist in a two-layer structure, i.e., microcells on the lower layer and macrocells (umbrella) in the upper layer. Within these systems, different types of handover have to be managed between the umbrellas and the microcells. In order to minimize the number of handovers, the MS velocity can be used in a cell layer assignment strategy, in which an MS is allocated to different hierarchical layers according to its velocity. The umbrella cells are used for fast-moving users and

[1] The distortions of the mobile communications channel are reviewed in Section 5.2.

[2] Handover or handoff is the process of transferring the control of a mobile station from one base station or channel to another. It is an essential component of mobile communications systems.

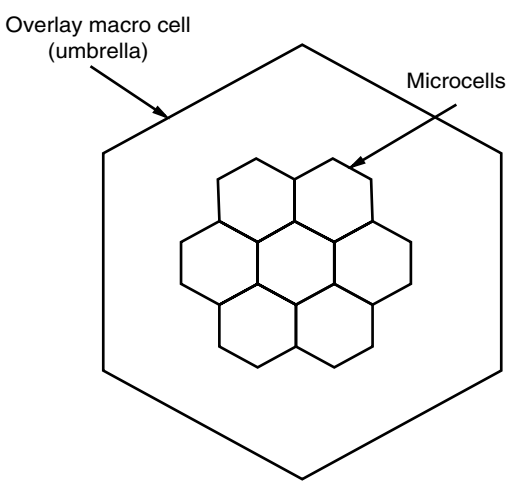

FIGURE 5.1 A multitier (microcell/macrocell overlay) system.

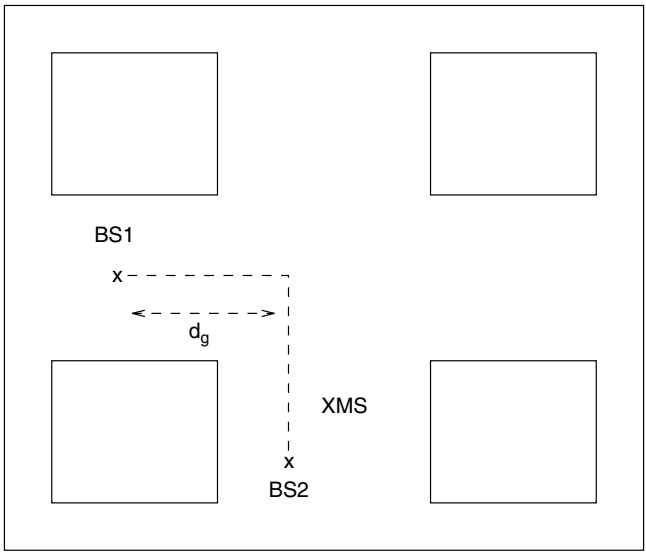

FIGURE 5.2 Corner effect: the MS turns round a corner, the LOS from the current BS (BS1) is lost, and an LOS is established between the MS and the target BS (BS2).

microcells for slow-moving users. This results in a reasonable grade of service (GoS) for both microcellular and multitier systems [33].

Reliable estimates of the MS velocity are also useful for effective dynamic channel assignment and the optimization of adaptive multiple-access wireless receivers [26, 69]. Since the performance of many receiver techniques depends on the fading rate of the received signal, an adaptive communications receiver can improve the performance and reduce the complexity of current systems by using Doppler information to control the receiver parameters. These parameters include the pilot filter bandwidth, the automatic gain control

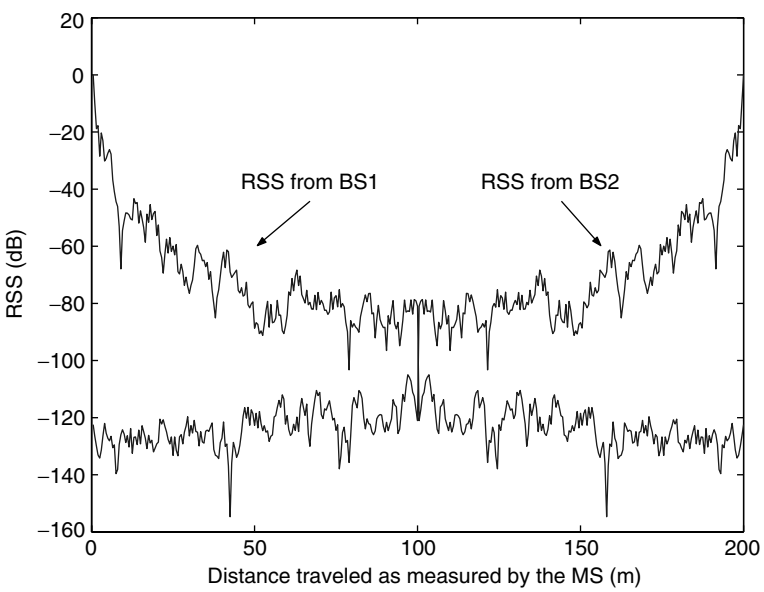

FIGURE 5.3 Received signal strength (RSS) at the MS from two neighboring BSs as a function of distance.

loop bandwidth, the phase tracker bandwidth, and the size of the interleaver [19, 52]. Based on this idea, Lee and Cho [42] proposed a power control scheme for codedivision multiple-access (CDMA) systems, which selects the power control step size based on the MS velocity. The MS velocity also affects the performance of a communications system operating in a pseudonoise (PN) tracking in CDMA systems [20, 22].

Mobile velocity estimation can occur at both BS and MS sites. For example, in the current CDMA 2000 system, the BS is responsible for power control [4, 41], and velocity is therefore estimated by the BS. However, a decision to hand off is made by the MS, and the MS is then responsible for estimating the velocity. Velocity estimation is performed by exploiting the statistics of a received pilot signal. For example, in CDMA 2000 the pilot signal consists of a constant-amplitude, zero-phase signal, spread by an all-one code sequence. It is then added to the information signal spread by an orthogonal sequence. The combination of the two signals is modulated by a carrier frequency and transmitted [21]. This process is equivalent to transmitting a pure carrier of constant amplitude alongside the information signal. At the reception, the combination of the two signals is demodulated, then correlated by each spreading sequence. Assuming no loss of orthogonality, the correlation of the received signal with the all-one sequence cancels the information signal and reveals the distortions introduced by the channel on the pilot signal.

5.1.2 Existing Velocity Estimators

Several mobile velocity estimators have been proposed in the literature, and some have been reviewed in [65]. Among the existing estimators are the zero-crossing rate of the in-phase or quadrature component [7], level crossing rate [7], and the autocovariance of the envelope of the received signal [5]. In [30, 31], the received signal samples are used to estimate the autocovariance function of the received faded envelope, from which the velocity information is extracted. Similarly, in [61], two methods for approximating the mobile velocity are proposed, based on the autocovariance function of the envelope and quadrature components of the received signal. The method proposed in [55] is based on the squared deviations of the logarithmically compressed signal envelope. In [1], the rate of maxima of the envelope of the received signal is used as a velocity estimator. The method in [49] is based on the estimator proposed in [1] and applies the continuous wavelet transform to locate the extrema of the received signal envelope. In [66], velocity estimators are derived, based on the spectral moments of the received signal. The method described in [36] uses the switching rate of diversity branches in a selection diversity combiner to estimate the MS velocity. In [68], mobile velocity is estimated by applying an eigenmatrix pencil method to the received signal samples. In [71], two methods are proposed for estimating mobile velocities for Global System for Mobile Communications (GSM) radios. The methods are based on estimating the deviation of the received signal strength. The method proposed in [50] uses the local stationarity of the received signal and expands it on a basis of smooth local complex exponentials. Velocity estimates have also been obtained by estimating the maximum Doppler frequency using eigenspace methods [6]. The method is designed under specific assumptions of the angular distribution of the incident power. Other velocity estimators have been proposed that require prior estimation of the channel [40] and covariance function of the channel power [48]. In [28], multiple BS and multidimensional scaling are used to estimate the velocity. This method requires knowledge of the average signal strength for all locations. In [26], a maximum likelihood estimator is derived and requires prior estimation of the channel parameters. A few estimators have also been proposed, which do not provide an explicit formula for the MS velocity, but rather classify the MS velocity as being fast, medium, or slow [39, 73, 74].

It was shown in [10, 11] that since all the above-mentioned techniques are based on the statistics of either the envelope or quadrature components of the received signal, they are not robust to shadowing. Other estimators have been proposed in [8, 9] based on the instantaneous frequency (IF) of the received signal. Recent work has already exploited the concept of IF estimation and time–frequency signal processing in wireless communications, e.g., in blind source separation, channel coding and capacity, interference excision, multiuser detection, code design, multicarrier transmission, and synchronization [2, 3, 12, 13, 17, 27, 35, 37, 38, 56, 57, 58, 59, 60, 72], and led to significant improvement in the systems [16, Chapter 13]. As shown in [9], the main advantage of IF-based velocity estimators is that they are robust to shadowing.

5.1.3 Structure of the Chapter

The chapter is structured as follows. Section 5.2 focuses on the received signal model in a mobile communications environment. In Section 5.3, we explain the principles behind velocity estimation and provide examples selected from the above-mentioned list of velocity estimators. The examples are selected on a basis of simplicity and performance. Section 5.4 provides the framework for analyzing the performance of velocity estimators with application to one specific estimator. In Section 5.5, we present simulation results of a selection of velocity estimators. Because some velocity estimators require prior knowledge of the Rice factor, we derive in Section 5.6 two Rice factor estimators. Section 5.7 discusses the importance of accurate velocity estimation in the context of handover decision algorithms, and Section 5.8 concludes this chapter.

5.2 Received Signal Model and Statistics

5.2.1 Received Signal Model

Propagation, in a mobile communications environment, is subject to three phenomena: path loss, shadowing, and multipath fading [62, p. 16]. Path loss affects all radio communications and refers to the loss of received power as the MS travels away from the BS. Path loss is completely characterized by the distance between the BS and the MS, the operating wavelength, the antenna height, and the surrounding terrain [62, p. 16]. Shadowing, or shadow fading, is caused by terrain configurations between the BS and MS and is produced by variations of the average of the envelope of the received signal over a few wavelengths. It is a random process and follows a lognormal distribution, i.e., when expressed in decibel, its distribution is Gaussian [62, p. 87]. Multipath fading, also referred to as fast fading, is due to the constructive and destructive superposition of many reflected, scattered, and diffracted plane waves arriving at the MS with different time delays and phase shifts. Figure 5.4 represents a typical received pilot signal envelope.

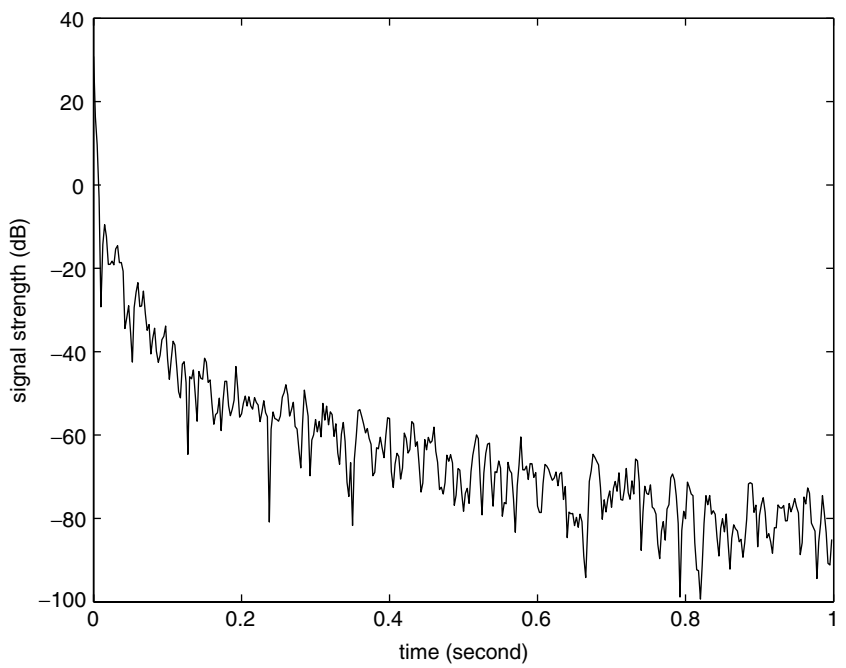

FIGURE 5.4 Typical received signal strength at an MS traveling at $v = 50$ km/h.

We assume, in what follows, that the distortions introduced by the channel are described by the model proposed by Lee and Yeh [44]. In this model, the real signal $y(t)$ received by an MS (or a BS) is the product of path loss, shadowing, and multipath fading with some additive noise:

$$\begin{aligned} y(t) &= m(t)s(t) + n(t) \\ &= p(t)m_o(t)s(t) + n(t) \end{aligned} \tag{5.1}$$

where $s(t)$ represents the multipath fading, $m_o(t)$ is the lognormal shadowing given by [49],

$$m_o(t) = 10^{L(t)/20} \tag{5.2}$$

$L(t)$ is a zero-mean Gaussian process, and $p(t)$ represents the path loss given by [49]:

$$p(t) = P_o(vt + d_o)^{-\alpha/2} \tag{5.3}$$

P_0 accounts for antenna parameters, transmitted power, and other relevant system parameters; vt represents the distance between the BS and an MS traveling at velocity v at time t; d_o is the distance between the BS and MS at time $t = 0$; and α, the exponent of the distance dependence, reflects the amount of power loss as a function of distance. The additive noise, $n(t)$, is assumed bandpass Gaussian with one-sided power spectral density (PSD) $S_N(f)$ given by [7]:

$$S_N(f) = \begin{cases} \frac{N_0}{2} & : \quad |f - f_c| < \frac{B_0}{2} \\ 0 & : \quad |f - f_c| > \frac{B_0}{2} \end{cases} \tag{5.4}$$

where B_0 represents the system bandwidth and is chosen equal to $\frac{2v_{max}}{\lambda}$, where v_{max} is the maximum mobile velocity and λ is the operating wavelength. $\frac{2v_{max}}{\lambda}$ represents the maximum expected Doppler frequency over the range of velocities.

5.2.2 Multipath Component Model

The multipath component, $s(t)$, is a result of the superposition of a number N of incoming waves, including a possible line-of-sight (LOS) component. Each incident wave $w_k(t)$ is modeled as a constant-amplitude, time-varying phase signal:

$$w_k(t) = \alpha_k e^{j(2\pi f_c t + \Phi_k(t))} \tag{5.5}$$

where α_k represents the amplitude of wave k and $\Phi_k(t)$ is the phase shift caused by the moving vehicle. If $w_k(t)$ arrives with angle of incidence θ_k with respect to the direction of travel of the MS, the Doppler shift created is

$$f_k = \frac{v}{\lambda} cos(\theta_k) \tag{5.6}$$

and the subsequent phase shift introduced by that wave is

$$\Phi_k(t) = 2\pi f_k t + \Psi_k = 2\pi \frac{v}{\lambda} cos(\theta_k)t + \Psi_k \tag{5.7}$$

If $w_k(t)$ is a LOS component, θ_k and Ψ_k are deterministic and depend on the position of the vehicle. Otherwise, θ_k and Ψ_k are random and are generally modeled as uniformly distributed between $(0, 2\pi)$ [34]. Combining Equation 5.5 and Equation 5.6, the multipath fading, $s(t)$, can be written as

$$s(t) = \Re \left\{ \sum_{k=1}^{N} w_k(t) \right\} \tag{5.8}$$

$$= \Re \left\{ e^{j2\pi f_c t} \left[\sum_{k=1}^{N} \alpha_k e^{j2\pi \frac{v}{\lambda} \cos(\theta_k)t + \Psi_k} \right] \right\} \tag{5.9}$$

where $\Re\{\}$ refers to the real-part operator, $w_1(t)$ is a possible LOS component, and $\{w_2(t), w_3(t) \ldots, w_N(t)\}$ are the result of $N-1$ independent scatterers and, as a consequence, are assumed independent and identically distributed (i.i.d). Signal $s(t)$ can be further written as

$$s(t) = s_i(t)\cos 2\pi f_c t - s_q(t)\sin 2\pi f_c t \tag{5.10}$$

where $s_i(t)$ and $s_q(t)$ are the respective in-phase and quadrature phase components of $s(t)$, defined as

$$s_i(t) = \sum_{k=1}^{N} \alpha_k \cos\left(2\pi \frac{v}{\lambda}\cos(\theta_k)t + \Psi_k\right) = x_i(t) + m_i \tag{5.11}$$

$$s_q(t) = \sum_{k=1}^{N} \alpha_k \sin\left(2\pi \frac{v}{\lambda}\cos(\theta_k)t + \Psi_k\right) = x_q(t) + m_q \tag{5.12}$$

where $E\{x_i(t)\} = E\{x_q(t)\} = 0$, $m_i = E\{s_i(t)\}$, $m_q = E\{s_q(t)\}$, and $E\{\}$ represents the expectation operator.

In the presence of a LOS component, the means m_i and m_q are nonzero [34] and

$$s(t) = (x_i(t) + m_i)\cos 2\pi f_c t - (x_q(t) + m_q)\sin 2\pi f_c t \tag{5.13}$$

$$= x(t) + m_i \cos 2\pi f_c t - m_q \sin 2\pi f_c t \tag{5.14}$$

where $x_i(t)$ and $x_q(t)$ are the respective in-phase and quadrature phase components of signal $x(t)$, i.e.,

$$x(t) = x_i(t)\cos 2\pi f_c t - x_q(t)\sin 2\pi f_c t \tag{5.15}$$

5.2.3 The Scattering Distribution

An important parameter in mobile communications system design is the distribution of incoming waves around a particular MS. It is referred to as scattering distribution. For example, in a typical macrocellular environment, the MS is usually uniformly surrounded by local scatterers, so that the plane waves arrive from many directions without an LOS component. As a consequence, the scattering distribution is usually considered isotropic. However, in a microcellular environment, the antennas of the BSS are only moderately elevated above the local scatterers. As a result, an LOS component may or may not exist and the scattering distribution is usually nonisotropic. The von Mises density provides a model for the distribution of the angle of arrival of the incoming waves [1, 45]. It is a function of one parameter, χ , which determines the directivity of the incoming waves. It is given by

$$p(\theta) = \frac{1}{2\pi I_0(\chi)} e^{\chi \cos\theta},\ \chi \geq 0,\ -\pi \leq \theta \leq \pi \tag{5.16}$$

where $I_n(.)$ is the modified Bessel function of order n and θ is the angle of incidence of the incoming waves. Figure 5.5 shows the polar plots of $p(\theta)$ against the angle of arrival of the plane waves for three different values of χ. It can be seen that for $\chi = 0$ the scattering distribution is isotropic and that it becomes more directive as χ increases.

5.2.4 Statistics of the Multipath Fading

When the number of incoming waves is sufficiently large (generally greater than six, [34, p. 69]), the in-phase and quadrature components of $x(t)$, defined in Equations 5.11 and 5.12, respectively, tend to be independent zero-mean Gaussian processes, with variance σ^2. As a consequence, the envelope of $s(t)$, defined as

$$|s(t)| = \sqrt{(x_i(t) + m_i)^2 + (x_q(t) + m_q)^2}$$

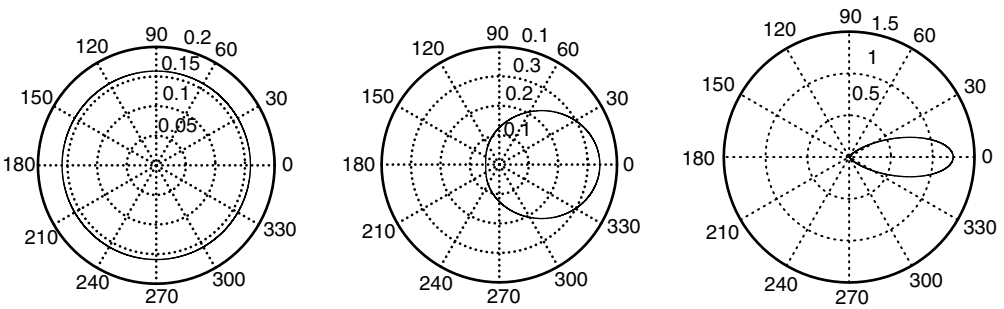

FIGURE 5.5 Polar plots of $p(\theta)$ in terms of θ for $\chi = 0$, $\chi = 1$, and $\chi = 10$. For $\chi = 0$ the scattering distribution is isotropic and becomes more directive as χ increases.

follows a Ricean distribution with Rice factor $K = \frac{\eta^2}{2\sigma^2}$, where $\eta^2 = m_i^2 + m_q^2$ [62, p. 518]. The Rice factor K represents the ratio of the power in the LOS component and scatter components of the signal $s(t)$.

The PSD of $x(t)$ is given in [62, p. 42] as

$$S_X(f) = \begin{cases} \frac{\sigma^2}{\sqrt{f_m^2 - (f - f_c)^2}} [G(\theta)p(\theta) + G(-\theta)p(-\theta)] & : \ |f - f_c| < f_m \\ 0 & : \ |f - f_c| > f_m \end{cases} \tag{5.17}$$

where $f_m = \frac{v}{\lambda}$ is the maximum Doppler frequency shift, $p(\theta)$ is the scattering distribution, and $G(\theta)$ is the gain of the MS antenna. We will assume in the remainder of the chapter that a vertical mono-pole antenna with $G(\theta) = \frac{3}{2}$ is used. Note that the PSD $S_X(f)$ is centered about the carrier frequency with a spectral width of $2f_m = \frac{2v}{\lambda}$.

Assuming the scattering distribution of equation 5.16, it can be shown that the n^{th} spectral moment of $x(t)$ is given by [1]

$$a_n = a_0(2\pi f_m)^n q_n(\chi) \tag{5.18}$$

where $a_0 = \frac{3}{2}\sigma^2$ and

$$q_n(\chi) = \frac{1}{\pi I_0(\chi)} \int_0^\pi e^{\chi \cos\theta} \cos^n \theta \, d\theta \tag{5.19}$$

Specifically, based on Equation 5.18 and Equation 5.19, we obtain

$$a_1 = a_0(2\pi f_m)\frac{I_1(\chi)}{I_0(\chi)} \tag{5.20a}$$

$$a_2 = a_0(2\pi f_m)^2 \left(\frac{I_0(\chi) + I_2(\chi)}{2I_0(\chi)}\right) \tag{5.20b}$$

In the case of isotropic scattering ($\chi = 0$), the first two spectral moments reduce to

$$a_1 = 0 \quad \text{and} \quad a_2 = 2a_0(\pi f_m)^2 \tag{5.21}$$

These statistics will be used further in the design of velocity estimators and in the evaluation of their performance.

5.3 Principles of Mobile Velocity Estimation

We can see from Equation 5.1 and Equation 5.9 that the information on mobile velocity is contained in both the envelope and phase of the received signal. The abundance of existing velocity estimators is a reflection of the numerous ways of extracting this information. The velocity of a mobile unit is generally estimated by exploiting the statistics of the envelope, phase, in-phase, and quadrature phase components or any other feature of the received signal. The approach for deriving a velocity estimator is based on the principle that there exists an exact, nonrandom relationship between the mobile velocity and the statistics of the Rician component $s(t)$ in the presence of isotropic scattering. Several exact and equivalent expressions of the velocity can be derived, depending on which feature of $s(t)$ is being considered, i.e., envelope, phase, in-phase, or quadrature phase, and which order of the statistic is chosen, i.e., first order, second order, etc. Below are some examples of these exact expressions of velocity.

5.3.1 Examples of Derivations of the Velocity

Below are some examples of how the mobile velocity can be calculated from the statistics of various features of $s(t)$.

Example 5.1 Level Crossing Rate Method

The envelope phase description of the Rician fading $s(t)$ is

$$s(t) = r(t)\cos(2\pi f_c t + \psi(t)) \tag{5.22}$$

where $r(t)$ and $\psi(t)$ represent the envelope and phase of $s(t)$, respectively.

The level crossing rate (LCR) is defined as the average number of upcrossings per second the envelope $r(t)$ makes of a predetermined level R_o. It is obtained as [43, p. 77]

$$LCR_r(R_0) = \int_0^\infty \dot{r}p(r = R_0, \dot{r})d\dot{r} = \frac{R_0}{a_0}\sqrt{\frac{a_2}{2\pi}}\exp\left(-\frac{R_0^2}{2a_0}\right) \tag{5.23}$$

where $p(r, \dot{r})$ denotes the joint probability density function (pdf) of $r(t)$ and its time derivative $\dot{r}(t)$, $a_0 = \frac{3}{2}\sigma^2$, and a_2 is the second spectral moment of $x(t)$, given in Equation 5.20b. If the level R_o is chosen equal to $\sqrt{2a_0}$, the LCR of level R_o becomes

$$LCR_r(R_0) = \sqrt{\frac{a_2}{\pi a_0}}\, e^{-1} \tag{5.24}$$

In the case of isotropic scattering, $a_2 = 2a_0(\pi f_m)^2$ (Equation 5.21). It follows that Equation 5.24 reduces to

$$LCR_r(R_0) = \sqrt{2\pi}\frac{\nu}{\lambda}\, e^{-1} \tag{5.25}$$

The mobile velocity can then be exactly expressed in terms of the average number of upcrossings the envelope $r(t)$ makes of level $R_o = \sqrt{2a_0}$ as

$$\nu = \frac{\lambda e}{\sqrt{2\pi}} LCR_r(R_0) \tag{5.26}$$

Example 5.2 Rate of Maxima Method

The rate of maxima (ROM) of a given process $r(t)$ is defined as the average number of maxima per second of $r(t)$. It can be derived as [53]

$$ROM_r = \int_0^\infty \ddot{r}\, p(\dot{r} = 0, \ddot{r})d\ddot{r} \tag{5.27}$$

where $p(\dot{r}, \ddot{r})$ denotes the joint (pdf) of the first and second derivatives of the process $r(t)$.

Using the results in [53], the ROM of the envelope $r(t)$ of signal $s(t)$ in Equation 5.22 can be obtained as

$$ROM_r = \frac{1.5651}{\pi}\sqrt{\frac{a_2}{2a_0}} \tag{5.28}$$

which, in the case of isotropic scattering, and following the approach of Example 1, reduces to

$$ROM_r = 1.5651\frac{\nu}{\lambda} \tag{5.29}$$

From Equation 5.29, the mobile velocity can then be exactly expressed in terms of the rate of maxima of the envelope of $s(t)$ as

$$\nu = 0.6389\lambda ROM_r \tag{5.30}$$

Example 5.3 Zero Crossing Rate Method

The zero crossing rate (ZCR) of a given process $a(t)$ is defined as the average number of positive-going zero crossings per second of that process. It is given by

$$ZCR_a = \int_0^\infty \dot{a}\, p(a = 0, \dot{a}) d\dot{a} \tag{5.31}$$

In [54], the ZCR definition was applied to the in-phase component of signal $x(t)$ defined in Equation 5.11 and Equation 5.15 and was shown to be equal to

$$ZCR_{x_i} = \frac{1}{2\pi}\sqrt{\frac{a_2}{a_0}} \tag{5.32}$$

which in the case of isotropic scattering reduces to

$$ZCR_{x_i} = \frac{\nu}{\sqrt{2}\lambda} \tag{5.33}$$

The mobile velocity can then be obtained using the following simple expression:

$$\nu = \sqrt{2}\lambda ZCR_{x_i} \tag{5.34}$$

The same result can be obtained using the quadrature component of $x(t)$ instead of the in-phase component.

Example 5.4 Covariance-Based Method

For the covariance (COV)-based method, consider a process $r_1(t) = r^2(t)$ where $r(t)$ is the envelope of the Rician fading $s(t)$. We can show that for a given time lag τ

$$E\{(r_1(t+\tau) - r_1(t))^2\} = 2R_{r_1}(0) - 2R_{r_1}(\tau) \tag{5.35}$$

where $R_{r_1}(\tau) = E\{r_1(t+\tau)r_1(t)\}$ is the autocorrelation function of process $r_1(t)$.

In [7], it was proved that in the presence of isotropic scattering

$$E\{(r_1(t+\tau) - r_1(t))^2\} \simeq R_{r_1}(0)\left(\frac{2\pi\tau_t\nu}{\lambda}\right)^2 \tag{5.36}$$

where τ_t is the sample spacing in seconds per sample and $R_{r_1}(0)$ is the variance of the squared envelope.

The mobile velocity can therefore be extracted from Equation 5.36 as

$$v = \frac{\lambda}{2\pi\tau_t}\sqrt{\frac{2R_{r_1}(0) - 2R_{r_1}(\tau)}{R_{r_1}(0)}} \tag{5.37}$$

where $R_{r_1}(\tau)$ is the autocorrelation of the envelope square $|s(t)|^2$ for a given time lag τ.

Example 5.5 Instantaneous Frequency-based Method

The IF of $s(t)$ is defined as [14]

$$f_{i,s}(t) = \frac{1}{2\pi}\frac{d\psi(t)}{dt} \tag{5.38}$$

where $\psi(t)$ is the phase of $s(t)$. In Appendix A, we show that the first moment of $|f_{i,s}|$ is

$$E\{|f_{i,s}|\} = \frac{v}{\sqrt{2}\lambda} I_0\left(\frac{K}{2}\right) e^{\frac{-K}{2}} \tag{5.39}$$

where $|\ |$ stands for the absolute value operator, $f_{i,s}$ is the IF of the multipath component $s(t)$, and K is the Rice factor. The velocity of a mobile unit can therefore be expressed in terms of the first-order moment of the absolute value of the IF of the Rician fading component $s(t)$ as

$$v = \sqrt{2}\lambda\ I_0^{-1}\left(\frac{K}{2}\right) e^{\frac{K}{2}} E\{|f_{i,s}|\} \tag{5.40}$$

5.3.2 Examples of Velocity Estimators

The expressions of the velocity in all the above examples are exactly equivalent. If we were to calculate the velocity using the LCR of the envelope of $s(t)$ (Equation 5.26) or the first-order moment of the IF of $s(t)$ (Equation 5.40), we would obtain exactly the same result. These exact expressions become estimators for two main reasons. The most important reason is that, in reality, we do not have access to $s(t)$, and the scattering distribution is not necessarily isotropic. The exact expressions obtained from exploiting the statistics of features of $s(t)$ in an isotropic environment become approximate in a nonisotropic environment, and in the presence of shadowing and additive noise. The second reason is that some parameters required to compute the exact expression of v must also be approximated. For example, in Equation 5.40, since exact values for $E\{|f_{i,s}|\}$ or K are not available, estimated values must be used, resulting in another source of error.

In the presence of shadowing, additive noise, and nonisotropic scattering, the previous exact expressions become the following estimators.

Example 5.1 LCR Estimator

From the expression of the velocity in Equation 5.26, we can derive an estimator

$$\hat{v}_{LCR} = \frac{\lambda e}{\sqrt{2\pi}} LCR_r(R_0) \tag{5.41}$$

where $LCR_r(R_0)$ represents the number of level of upcrossings of the envelope of $y(t)$ and where $\hat{R}_0 = \sqrt{2\hat{a}_0}$, with

$$\hat{a}_0 = \frac{1}{T}\int_T y_i^2(t)dt - \left(\frac{1}{T}\int_T y_i(t)dt\right)^2 \tag{5.42}$$

where $y_i(t)$ is the in-phase component of the received signal.

Example 5.2 ROM Estimator

From the expression of the velocity in Equation 5.30, we can derive an estimator

$$\hat{v}_{ROM} = 0.6389\lambda ROM_r \tag{5.43}$$

where ROM_r is the rate of maxima of the envelope of the received signal $y(t)$.

Example 5.3 ZCR Estimator

From the expression of the velocity in Equation 5.34, we can derive the following estimator:

$$\hat{v}_{ZCR} = \sqrt{2}\lambda ZCR_{z_i} \tag{5.44}$$

where ZCR_{z_i} is the zero crossing rate of $z_i(t) = y_i(t) - \bar{y}_i(t)$, where $y_i(t)$ is the in-phase component of the received signal $y(t)$ and $\bar{y}_i(t)$ an estimate of its mean.

Example 5.4 COV-Based Estimator

From the expression of the velocity in Equation 5.37, we can derive the following estimator:

$$\hat{v}_{COV} = \frac{\lambda}{2\pi\tau_t}\sqrt{\frac{\overline{V}}{R(0)}} \tag{5.45}$$

where τ_t is the sample spacing in seconds per sample, $R(0)$ is the variance of the envelope square of the received signal, and

$$\overline{V} = 2(R(0) - R(\tau)) \tag{5.46}$$

Example 5.5 IF-Based Estimator

The IF-based estimator is obtained from Equation 5.40 as

$$\hat{v}_{IF} = \lambda\sqrt{2}I_0^{-1}\left(\frac{\hat{K}}{2}\right)e^{\frac{\hat{K}}{2}} < |\hat{f}_{i,y}(t)| > \tag{5.47}$$

where

$$< |\hat{f}_{i,y}(t)| >= \frac{1}{T}\int_T |\hat{f}_{i,y}(t)|dt$$

is the time average of the IF estimate of the received signal over the duration T of the recorded signal, and $\hat{K}$ is the estimated Ricean factor.

All the above-mentioned and other existing estimators exhibit different performances in the presence of additive noise, shadowing, and nonisotropic scattering. For example, in the presence of shadowing, the envelope of $s(t)$ is distorted while its IF is not. As a consequence, any estimator based on the IF of the received signal would be expected to be more robust to shadowing than estimators based on the envelope of the received signal. The approach for evaluating the performance of velocity estimators is decribed in the next section.

5.4 Performance Analysis of Velocity Estimators

The examples of the previous section showed that several exact expressions of the velocity of a mobile unit can be obtained from exploiting different statistics and different features of the Rician component $s(t)$. In the presence of additive noise, shadowing, and a nonisotropic environment, these exact expressions are used as velocity estimators with different properties and performances. Any performance analysis of a velocity estimator should evaluate its behavior in the presence of shadowing, additive noise, and

nonisotropic scattering. This approach is illustrated below for the IF-based estimator but can be applied to any other estimator.

5.4.1 Effect of Shadowing

In this section, the effect of shadowing is studied in the absence of additive noise. The model for the received signal is therefore $y(t) = m(t)s(t)$. We observe that $m(t)$ causes a distortion in the amplitude and quadrature components of the received signal. Thus, the performance of all velocity estimators that are based on the statistics of the envelope and quadrature components of the received signal deteriorates in the presence of shadowing. However, since the presence of shadowing changes only the amplitude of the received signal [43, p. 203; 62, p. 91], it produces no phase distortion. Hence, the IF of the received signal is not affected by $m(t)$; i.e., both signals $s(t) = r(t)\cos(2\pi f_c t + \psi(t))$ and $y(t) = m(t)r(t)\cos(2\pi f_c t + \psi(t))$ have the same IF, $\frac{1}{2\pi}\dot{\psi}(t)$. The IF-based estimator is therefore robust to shadowing and to any other amplitude distortion, such as path loss.

5.4.2 Effect of AWGN and Nonisotropic Scattering

5.4.2.1 Derivation of the Normalized Bias

In this section, the performance of the IF-based estimator is investigated in the presence of additive white Gaussian noise (AWGN), nonisotropic scattering, and the absence of shadowing. The performance criterion is the normalized bias of the estimator. Ideally, the variance of the estimator should also be derived. However, at the time of publication, there is no closed-form expression of the variance. This is also the case for all existing estimators. The variance will be investigated in the next section using Monte Carlo simulations.

The normalized bias of estimator $\hat{v}_{IF}$ in Equation 5.47 is defined as

$$\begin{aligned}\varepsilon(\chi, \gamma, K) &= \frac{\hat{v}_{IF}}{v} - 1 \\ &= \frac{\sqrt{2}\lambda}{v} I_0^{-1}\left(\frac{K}{2}\right) e^{\frac{K}{2}} E\{|f_{i,y}|\} - 1\end{aligned} \tag{5.48}$$

where γ is the signal-to-noise ratio (SNR) and

$$E\{|f_{i,y}|\} = \frac{1}{2\pi}\int_{-\infty}^{\infty} |\dot{\psi}|\, p(\dot{\psi})\, d\dot{\psi} \tag{5.49}$$

$p(\dot{\psi})$ is given by [54]

$$\begin{aligned}p(\dot{\psi}) = \frac{1}{8a}\sqrt{\frac{2}{ab_0\mathcal{B}}} \exp\left(\frac{b_1^2\rho + c\mathcal{B}}{2\mathcal{B}} - \frac{b_0 b_2 \rho}{\mathcal{B}}\right) \\ \times \left[(c+1)\, I_0\left(\frac{c\mathcal{B} - b_1^2\rho}{2\mathcal{B}}\right) + c\, I_1\left(\frac{c\mathcal{B} - b_1^2\rho}{2\mathcal{B}}\right)\right]\end{aligned} \tag{5.50}$$

where

$$\rho = \frac{Q^2}{2b_0} \tag{5.51}$$

with $Q^2 = \frac{3}{2}M^2\eta^2$

$$\mathcal{B} = b_0 b_2 - b_1^2 \tag{5.52a}$$

$$a = \frac{b_2 - 2b_1\dot{\psi} + b_0\dot{\psi}^2}{2\mathcal{B}} \tag{5.52b}$$

$$c = \frac{Q^2(b_2 - b_1\dot{\psi})^2}{4a\mathcal{B}^2} \tag{5.52c}$$

and b_n is the n^{th} spectral moment of $y_0(t) = m(t)x(t) + n(t)$. $y_0(t)$ is the received signal in the absence of an LOS component.

In the absence of shadowing, $m(t)$ is a constant M. Since both $x(t)$ and $n(t)$ are zero-mean, independent processes, the n^{th} spectral moment of $y_0(t)$ can be written as

$$\begin{aligned} b_n &= (2\pi)^n \int_0^\infty (f - f_c)^n (M^2 S_X(f) + S_N(f)) df \\ &= M^2 a_n + (1 - (-1)^{n+1}) \frac{N_0 \pi^n}{4(n+1)} B_0^{n+1}, \\ & n \geq 0 \end{aligned} \tag{5.53}$$

5.4.2.2 Performance in the Presence of AWGN and Isotropic Scattering

In the case of isotropic scattering ($\chi = 0$, Figure 5.5(a)), $E\{|f_{i,y}|\}$ is given by (Equation 5.A5)

$$E\{|f_{i,y}|\} = \frac{1}{2\pi} \sqrt{\frac{b_2}{b_0}} \exp\left(\frac{-\rho}{2}\right) I_0\left(\frac{\rho}{2}\right) \tag{5.54}$$

The normalized bias of Equation 5.48 can then be written as

$$\varepsilon(0, \gamma, K) = \frac{\lambda}{\sqrt{2}\pi\nu} \sqrt{\frac{b_2}{b_0}} I_0\left(\frac{\rho}{2}\right) I_0^{-1}\left(\frac{K}{2}\right) e^{\frac{K-\rho}{2}} - 1 \tag{5.55}$$

where ρ is defined in Equation 5.51. After using Equation 5.18 and Equation 5.53, Equation 5.55 becomes

$$\varepsilon(0, \gamma, K) = \sqrt{\frac{\gamma + \frac{1}{6}(\frac{\lambda B_0}{\nu})^2}{\gamma + 1}} I_0\left(\frac{K\gamma}{2(\gamma+1)}\right) I_0^{-1}\left(\frac{K}{2}\right) e^{\frac{K}{2(\gamma+1)}} - 1 \tag{5.56}$$

Figure 5.6 and Figure 5.7 show the effect of AWGN on the IF-based estimator with respect to γ and ν, for two different values of K. The bandwidth B_0 is assumed to be $B_0 = \frac{2\nu_{max}}{\lambda} = 170$ Hz, which allows

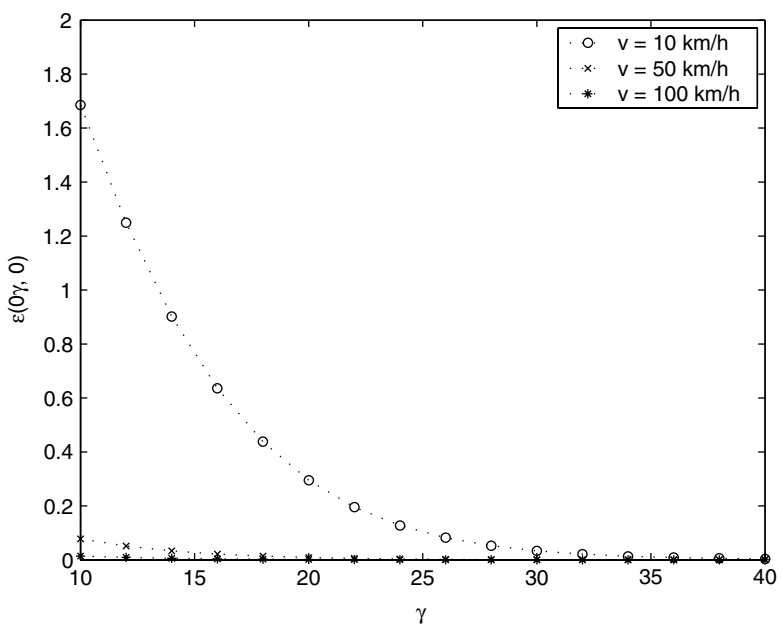

FIGURE 5.6 The normalized bias of the IF-based velocity estimator as a function of SNR for three different MS velocities, assuming $K = 0$.

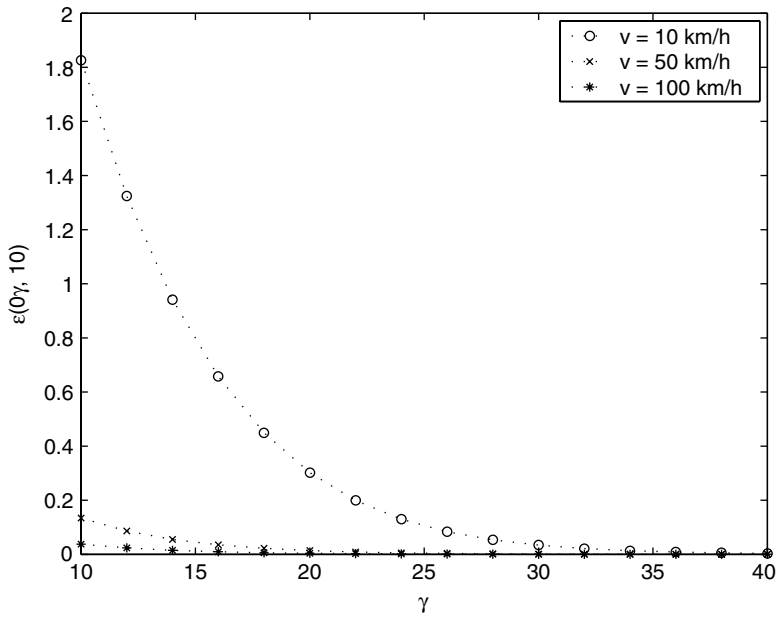

FIGURE 5.7 The normalized bias of the IF-based velocity estimator as a function of SNR for three different MS velocities, assuming $K = 10$.

for velocities up to $v_{max} = 100$ km/h at $f_c = 900$ MHz. We observe that for low velocities and low SNR, the bias is significant. The normalized bias is also seen to increase slightly as K increases. This is also the case for some existing estimators [7]. However, Appendix C shows that the IF estimator allows for an improvement in SNR by a factor of $3 \ln \frac{B_0}{2 f_1}$, where f_1 is the lower cutoff frequency of the output low-pass filter at the output of the IF estimator. For typical values, $B_0 = 170$ Hz and $f_1 = 10$ Hz, the improvement is about 8 dB. This means that the normalized bias of the IF-based estimator for an input SNR of 10 dB is the same as that of the ZCR method for an input SNR of 18 dB. Thus, even for small velocities, the IF-based estimator will still exhibit a negligible bias at low SNRs due to the improvement of SNR at the output of the IF estimator.

5.4.2.3 Performance in the Presence of Nonisotropic Scattering and in the Absence of AWGN

The effect of the scattering distribution is investigated here in the absence of noise ($\gamma \to \infty$). In this case, using Equation 5.50, the normalized bias in Equation 5.48 in the absence of additive noise, $\varepsilon(\chi, \infty, K)$, can be computed numerically. Figure 5.8 shows the effect of the scattering distribution on the IF-based estimator for different values of χ. Because the estimator in Equation 5.47 was derived in the case of isotropic scattering, the error in estimating the MS velocity increases as χ increases. Comparing Figure 5.8(a) and (b), we observe that there is a negligible increase in normalized bias when K increases. This suggests that $\varepsilon(\chi, \infty, K)$ can be approximated by $\varepsilon(\chi, \infty, 0)$. Using Equation 5.48 and Equation 5.A5, we obtain

$$\begin{aligned} \varepsilon(\chi, \infty, K) &\simeq \varepsilon(\chi, \infty, 0) \\ &= \sqrt{2\, q_2(\chi)} - 1 \end{aligned} \tag{5.57}$$

Appendix B shows that the ZCR-based velocity estimator (Equation 5.44) has the same normalized bias as the IF-based estimator (Equation 5.47) in the presence of nonisotropic scattering. The ZCR-based velocity estimator is generally more robust than the LCR and covariance-based methods in the presence of nonisotropic scattering [7]. It then follows that the IF-based velocity estimator also outperforms the above-mentioned estimators in the presence of nonisotropic scattering.

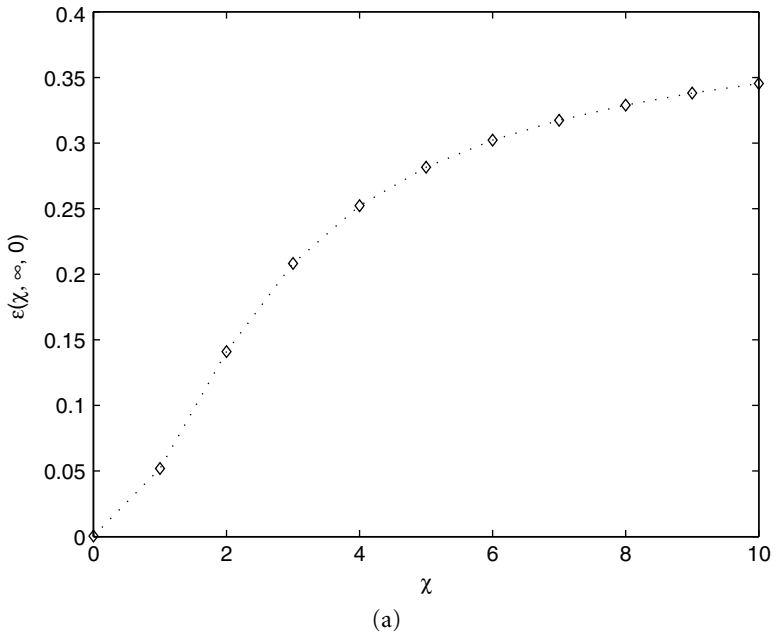

(a)

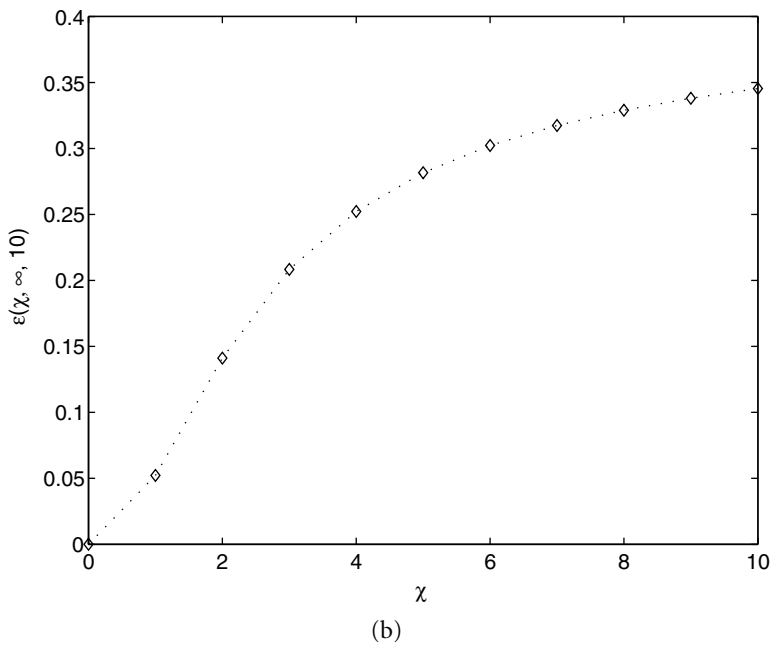

(b)

FIGURE 5.8 The normalized bias of the IF-based velocity estimator as a function of χ: (a) for $K = 0$ and $v = 40$ km/h, (b) for $K = 10$ and $v = 40$ km/h.

In summary, unlike the ZCR, LCR, and COV-based methods, or any method based on the envelope, in-phase, or quadrature phase of the received signal, the IF-based velocity estimator is robust to shadowing. It also exhibits superior performance in the presence of AWGN due to the improvement in SNR introduced by the IF estimator. In the presence of nonisotropic scattering, the IF-based estimator has the same performance as the ZCR and is generally more robust than LCR and COV-based methods. The effects of additive noise, nonisotropic scattering, and shadowing combine in a nonlinear way and are easier to evaluate using simulations. This is the object of the next section.

5.5 Performance Analysis Using Simulations

In Section 5.4, the performance of the IF-based estimator was evaluated analytically in the case of restrictive assumptions. For example, the IF-based estimator was evaluated in terms of the bias introduced in the presence of additive noise, shadowing, and nonisotropic scattering considered separately. It is also important to investigate the performance of an estimator when all these effects are present at once, which is the case in real life. Analytical derivations can, in that case, become intractable, and it is often easier to use simulations. Also, the IF-based estimator was evaluated in terms of bias only. However, the variance of an estimator is another important measure of performance. At time of publication, in the case of the IF-based estimator or any other velocity estimator, there is no closed-form expression for the variance. In this case, Monte Carlo simulations are used. Finally, the analytical derivations of Section 5.4 assumed perfect knowledge of the first-order moment of the IF of the received signal and of the Rice factor. A more accurate performance study would require taking into account the statistics of the estimators used for the first order of the IF and for the Rice factor. However, the derivations would again become too complex and simulations are a better alternative.

5.5.1 Simulations of the Received Signal

Using Jakes method for simulating the multipath component of the received signal, the in-phase and quadrature components of $x(t)$ defined in Equation 5.15 can be modeled as [34]

$$x_i(t) = \sum_{n=1}^{N} \cos\left(2\pi f_m t \cos\left(\frac{2\pi n}{N}\right) + \Psi_n\right) \tag{5.58a}$$

$$x_q(t) = \sum_{n=1}^{N} \sin\left(2\pi f_m t \cos\left(\frac{2\pi n}{N}\right) + \Psi_n\right) \tag{5.58b}$$

where N is the number of waves arriving at the MS antenna and $\Psi_n (n = 1, 2, \ldots, N)$ are assumed to be i.i.d. uniformly on $(0, 2\pi)$. The process $L(t)$ of Equation 5.2 is modeled as a zero-mean Gaussian process with PSD $S_L(\nu)$ given by

$$S_L(\nu) = \frac{2d_0\sigma_L^2}{1 + (2\pi\nu d_0)^2} \tag{5.59}$$

where d_0 and σ_L^2 are the correlation length and variance of L, respectively. Let ν_{max} denote the maximum spatial frequency of $S_L(\nu)$, and $D = \nu T$, with T the total duration of the simulated signal. A model for L is [49]

$$L(t) = \sum_{k=-J}^{J-1} \left[\frac{2}{CD} S_L\left(\frac{k + 1/2}{D}\right)\right]^{\frac{1}{2}} \times \cos\left(\frac{2\pi t}{T}(k + 1/2) + \theta_k\right) \tag{5.60}$$

where $\theta_k (k = -J, -J + 1, \ldots, J)$ are assumed to be i.i.d. uniformly on $(0, 2\pi)$, $J = D\nu_{max}$, and

$$C = \frac{1}{D\sigma_L^2} \sum_{k=-J}^{J-1} S_L\left(\frac{k + 1/2}{D}\right) \tag{5.61}$$

In these simulations, the carrier wavelength is $\lambda = 1/3$ ($f_c = 900$ MHz), and the exponent of the distance dependence is $\alpha = 2$. The standard deviation of lognormal shadowing ranges from 6.5 to 8.2 dB at 900 MHz in urban areas for microcells [47]. Here, the standard deviation and correlation length of the lognormal shadowing are $\sigma_L = 8$ dB and $d_0 = 50$ m, respectively. Parameter P_0 is assumed equal to 1 W.

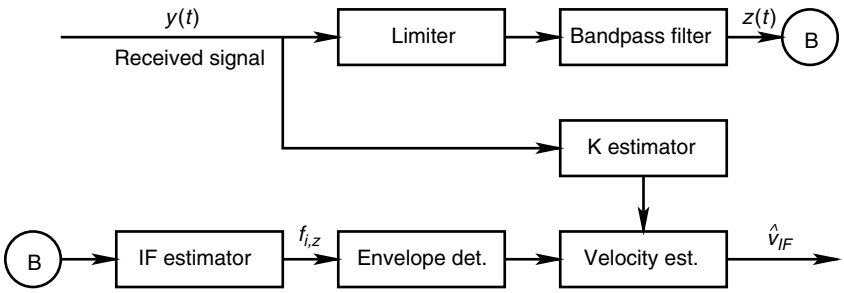

FIGURE 5.9 Block diagram of the IF-based MS velocity estimator.

5.5.2 Simulation Results

We consider that only a finite duration of the received signal is observed, and that the IF and moments of the signal are estimated using a finite duration of the received signal. The performance of the IF-based estimator is then compared with that of other estimators.

For each value of the MS velocity, the estimator $\hat{v}_{IF}$ in Equation 5.47, is computed by using the approach illustrated in Figure 5.9. A limiter is used to remove spurious amplitude variations from the received signal without destroying the information in the phase. It is followed by a bandpass filter of suitable bandwidth B_0, in order to extract the constant-amplitude signal. A value of $B_0 = 170$ Hz is chosen for the system bandwidth. This process is widely used in FM receivers [18, pp. 205–207]. The signal $z(t)$ is a constant-amplitude frequency-modulated signal and can be expressed as

$$z(t) = A\cos(2\pi f_0 t + \phi(t)) + n_o(t) \tag{5.62}$$

where A is the maximum amplitude at the limiter output and $n_o(t)$ is the bandpass noise at the output of the filter. The IF of the signal $z(t)$ can be estimated using [15]

$$f_{i,z}(t) = \frac{1}{2\pi}\frac{z_i(t)z_q'(t) - z_i'(t)z_q(t)}{z_i^2(t) + z_q^2(t)} \tag{5.63}$$

with $z_i(t) = A\cos(\phi(t)) + n_{oi}(t)$ and $z_q(t) = A\sin(\phi(t)) + n_{oq}(t)$. In practice, however, this method is difficult to implement as coherent detectors are needed to recover the in-phase and quadrature components of $z(t)$. In order to overcome this problem, a balanced discriminator can be deployed to estimate the IF of $z(t)$ [18, p. 216]. This is the method used in these simulations. The samples of the signal $z(t)$ are passed through an finite impulse response (FIR) differentiator. The envelope of the output of the differentiator is proportional to $f_{i,z}(t)$. Therefore, unlike other estimators such as the ZCR estimator, the IF-based estimator does not require coherent detectors. The Ricean K factor is estimated using the estimator of Equation 5.70 derived in the next section. The IF-based estimator of Equation 5.47 can then be calculated using the envelope of the estimated IF and the estimated K factor.

The performance of the IF-based estimator in the presence of shadowing and additive noise was compared with that of the ZCR, LCR, ROM, and COV-based methods by computing the average normalized bias and variance over 100 realizations of the received signal. The sensitivity of the COV-based method to additive noise can be reduced significantly by choosing a large time lag. However, a large time lag reduces the accuracy of the estimator itself. Here, the time lag in the COV-based method was chosen to be 2.5 msec, which according to our simulations gives an accurate estimate of the MS velocity in the ideal case. In order to limit the delay in obtaining velocity estimates for real-time implementation, we used a window of 1 sec of the simulated signal to estimate the unknown velocity. As the window length increases, the bias introduced by estimating $E\{|f_{i,y}|\}$ using the time average of the estimated IF decreases, and the delay in obtaining velocity estimates increases.

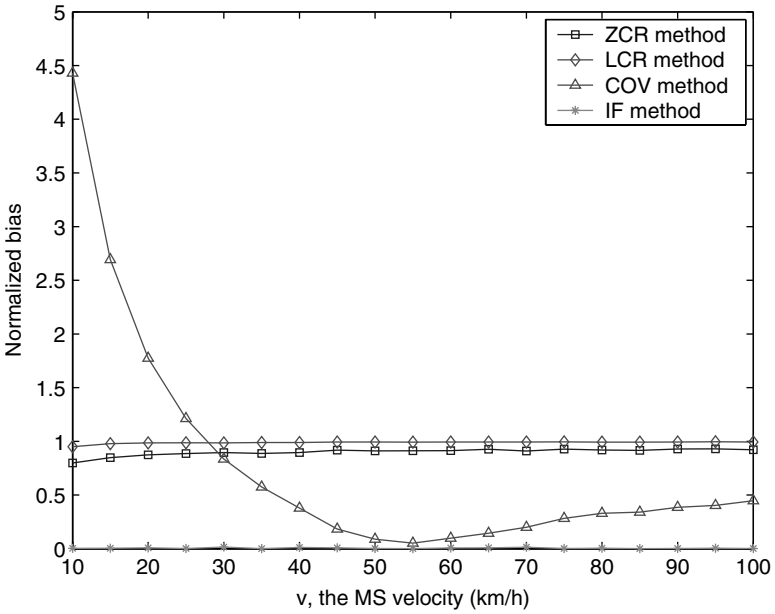

FIGURE 5.10 Normalized bias as a function of the MS velocity in the presence of shadowing.

Figure 5.10 shows the effect of shadowing on each of the velocity estimators in the absence of additive noise and in the case of isotropic scattering. We observe that in the presence of shadowing, the normalized bias in estimated velocity for the IF-based estimator is negligible compared to the other estimators. This confirms that the IF-based estimator is robust to shadowing.

Figure 5.11 shows the effect of additive noise in the absence of shadowing, assuming isotropic scattering. We observe that the IF-based estimator is generally more robust than the other estimators. It exhibits a

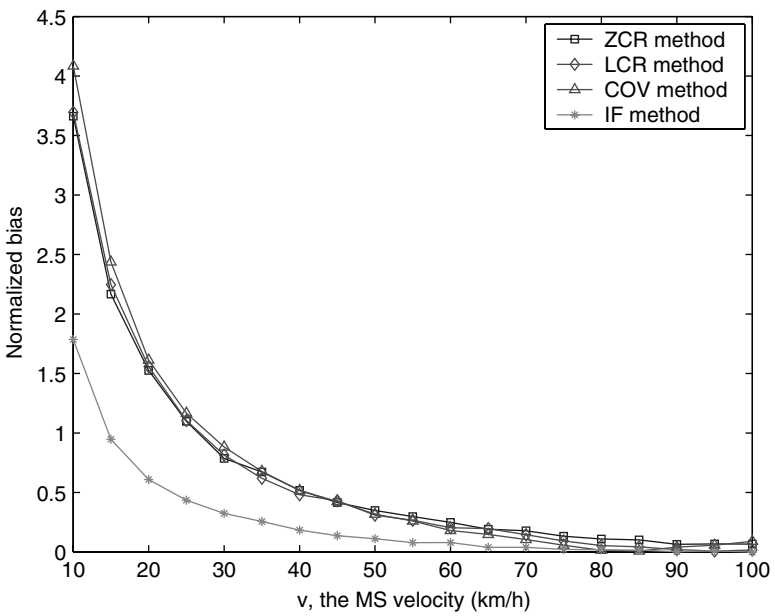

FIGURE 5.11 Normalized bias as a function of the MS velocity in the presence of AWGN for SNR = 10 dB.

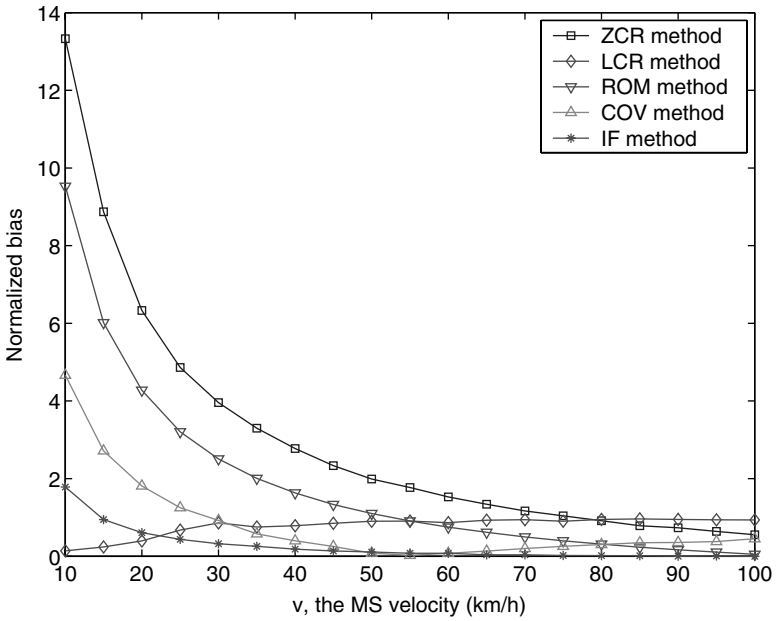

FIGURE 5.12 Normalized bias as a function of the MS velocity in the presence of AWGN, shadowing, and isotroic scattering for SNR = 10 dB.

smaller bias than the other estimators for small velocities. This is due to the improvement in SNR at the output of the IF estimator (see Appendix C). As the MS velocity increases, the system bandwidth approaches the actual Doppler shift, and therefore, the difference between the normalized biases of all the estimators becomes particularly small. Finally, Figure 5.12 to Figure 5.14 represent the respective normalized bias,

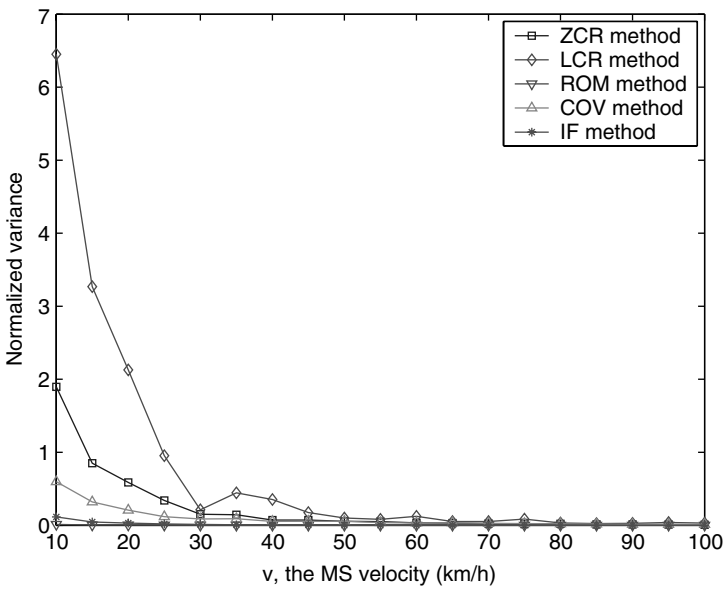

FIGURE 5.13 Variance as a function of the MS velocity in the presence of AWGN, shadowing, and isotroic scattering for SNR = 10 dB.

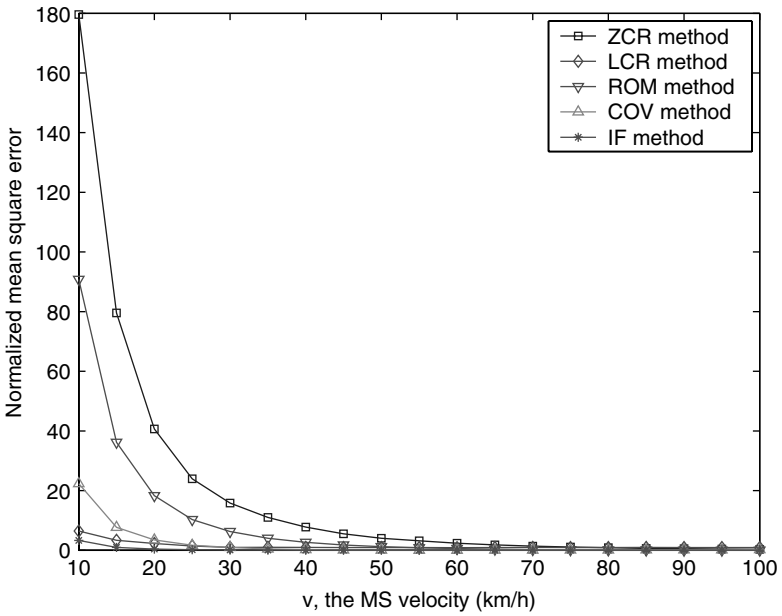

FIGURE 5.14 Mean square error as a function of the MS velocity in the presence of AWGN, shadowing, and isotropic scattering for SNR = 10 dB.

the variance, and the mean square error of the above-considered estimators in the presence of additive noise, shadowing, and isotropic scattering. They indicate that the ROM estimator exhibits slightly lower variance than the IF-based estimator, but higher bias and mean square error.

5.6 Rice Factor Estimation

5.6.1 Existing Methods

The value of K influences most local power and mobile velocity estimators [7]. It is also a measure of the severity of the fading, $K = 0$ being the most severe Rayleigh fading and $K = \infty$ indicating that there is no fading. Hence, knowledge of the Ricean K factor is a good indicator of the channel quality [25].

Traditional methods for estimating the Ricean K factor are based on measurements of the received power. In [25], the probability distribution of the measured data is computed and compared to a set of hypothesis distributions using a suitable goodness-of-fit test. In [46], a maximum likelihood estimate of K is obtained using an expectation–maximization (EM) algorithm. Both methods have a high degree of complexity, which makes them relatively time-consuming [24]. A simple and rapid method for K estimation uses two estimated moments of the received power [24]. The same estimator has been derived in [66] using an approach based on the covariance of the received power. In [63], the Ricean K factor is estimated using the first two moments of the envelope of the received signal. However, this method did not receive much attention, as it did not provide a closed-form expression for K. However, Tepedelenlioğlu et al. [64] recently proposed a general class of moment-based estimators for K, which included the estimator of [63]. They derived the asymptotic variance of each member of the family and showed that the asymptotic variance of the estimator in [63] is the closest to the Cramer–Rao lower bound. In this section, we present two explicit and simple estimators for K based on an approximation of the method in [63]. We also show, using simulations, that one of the proposed estimators has a lower mean square error than the estimator in [24] and [66].

5.6.2 Envelope-Based Estimators

The ratio of the first two moments of the envelope, $r(t)$, of the Rician fading is [53]

$$E_r \triangleq \frac{E\{r\}}{\sqrt{E\{r^2\}}} = \frac{\sqrt{\pi}e^{-\frac{K}{2}}}{2\sqrt{K+1}}\left[(1+K)I_0\left(\frac{K}{2}\right) + KI_1\left(\frac{K}{2}\right)\right] \tag{5.64}$$

Using Equation 5.64, $\hat{K}$ can be obtained by first estimating the first two moments of $r(t)$, and then solving Equation 5.64 numerically for K. This was the method originally proposed in [63]. However, since Equation 5.64 does not provide an explicit formula for K, it has not been used as an estimator.

To overcome the aforementioned drawback, we approximate the right side of Equation 5.64, and derive two explicit estimators for K. We first rewrite Equation 5.64 as

$$E_r = \frac{g(K)}{K+1} \tag{5.65}$$

where $g(K)$ is defined as

$$g(K) \triangleq \frac{\sqrt{\pi}}{2}e^{-\frac{K}{2}}\sqrt{K+1}\left[(1+K)I_0\left(\frac{K}{2}\right) + KI_1\left(\frac{K}{2}\right)\right] \tag{5.66}$$

Figure 5.15 plots $g(K)$ for $K \in [0, 100]$. It suggests that $g(K)$ can be well approximated with a low-order polynomial function $g_N(K)$, where

$$g_N(K) = \sum_{i=0}^{N} p_{iN}K^i \tag{5.67}$$

The coefficients p_{iN} $(i = 0, 1, \ldots, N)$ are computed by fitting $g_N(K)$ to $g(K)$ in a least squares sense. It can be shown that for $N > 2$, $p_{iN}, i > 2$ is of order 10^{-5}. We choose to approximate $g(K)$ with a linear and quadratic function, $g_1(K)$ and $g_2(K)$, respectively.

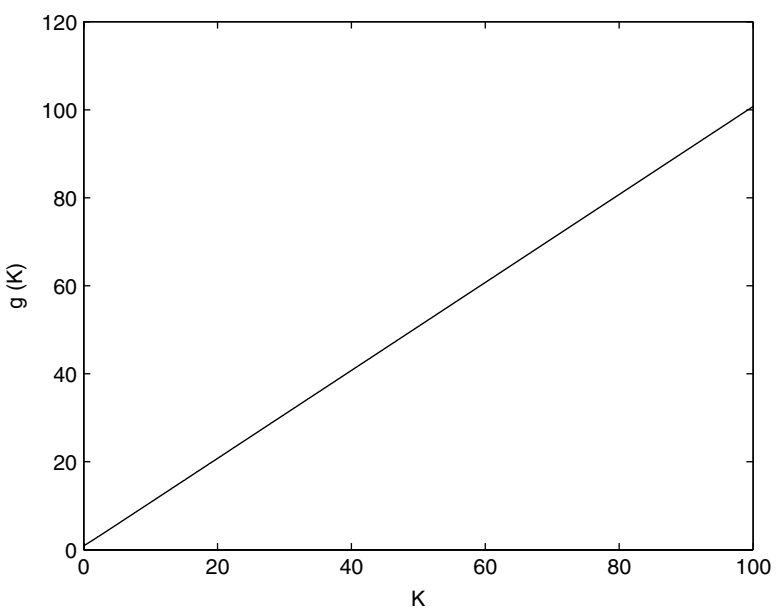

FIGURE 5.15 $g(K)$ in Equation 5.66 vs. K. We observe that $g(K)$ can be well approximated by a low-order polynomial.

Replacing $g(k)$ by its linear approximation in Equation 5.65 leads to the following estimator:

$$\widehat{K_1} = \frac{\widehat{E_r} - p_{01}}{p_{11} - \widehat{E_r}} \tag{5.68}$$

In Equation 5.68, $\widehat{E_r}$ is the ratio of the estimated first and second moments of the envelope of the received signal, i.e., $\widehat{E_r} = \overline{R}/\sqrt{\overline{R^2}}$ where, assuming local ergodicity,

$$\overline{R^n} = \frac{1}{T}\int_T R^n(t)dt, \quad n = 1, 2$$

and T is the duration of the observed signal. By fitting $g_1(K)$ to $g(K)$ in a least squares sense, we find

$$p_{01} = 0.7967, \; p_{11} = 0.9969 \tag{5.69}$$

Following the same approach, $g(k)$ is replaced by its quadratic approximation in Equation 5.65, which leads to the following estimator:

$$\widehat{K_2} = \frac{\widehat{E_r} - p_{12} + \sqrt{(\widehat{E_r} - p_{12})^2 + 4p_{22}(\widehat{E_r} - p_{02})}}{2p_{22}} \tag{5.70}$$

where

$$p_{02} = 0.8293, \; p_{12} = 0.9866, \; p_{22} = 0.0005 \tag{5.71}$$

Parameter E_r in Equation 5.64 can be approximated by

$$E_r \simeq E_{r1} = \frac{p_{01} + p_{11}K}{K + 1} \tag{5.72}$$

or

$$E_r \simeq E_{r2} = \frac{p_{02} + p_{12}K + p_{22}K^2}{K + 1} \tag{5.73}$$

depending on the degree of accuracy required.

Figure 5.16 plots Equation 5.64 and its approximations (Equation 5.72 and Equation 5.73). It verifies that E_{r2} is a better approximation than E_{r1}.

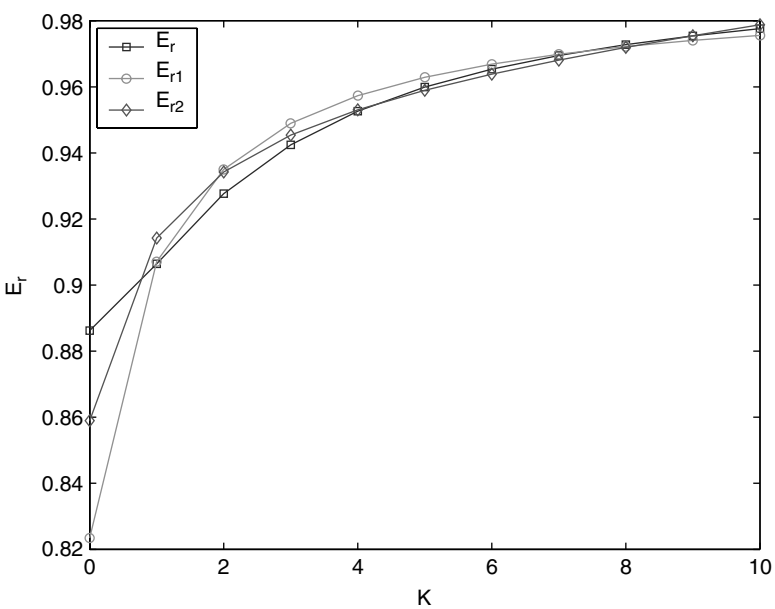

FIGURE 5.16 E_r vs. K (Equation 5.64) and its approximations (Equation 5.72 and Equation 5.73).

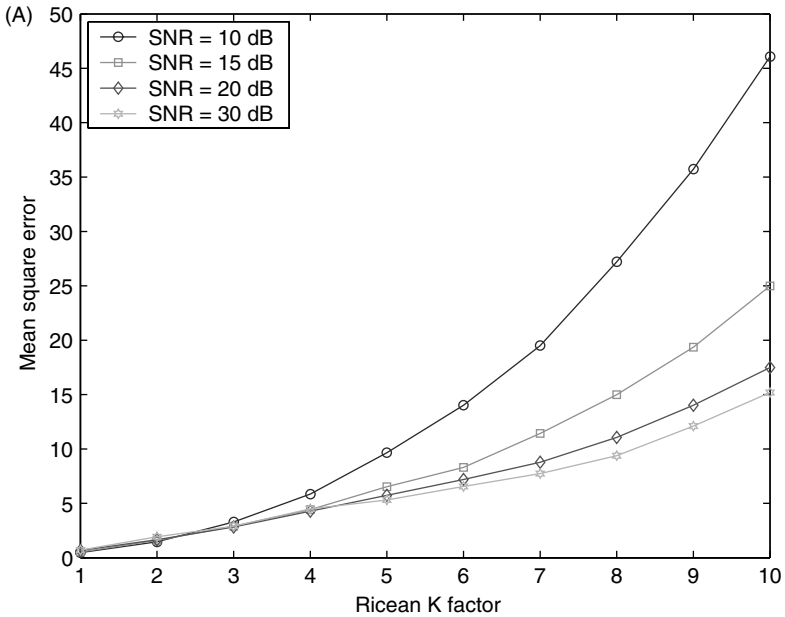

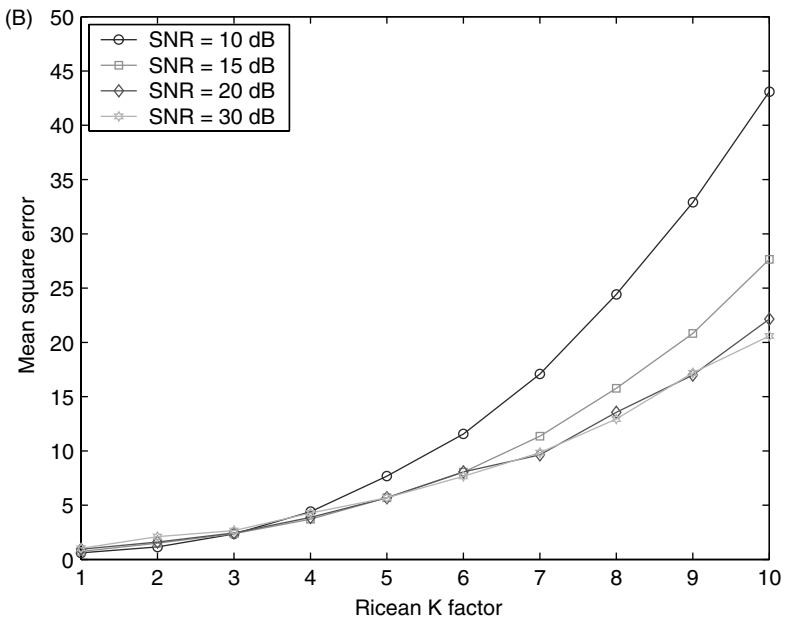

FIGURE 5.17 The MSE of the (A) estimator in Equation 5.70, (B) estimator in Equation 5.74, and (C) estimator in Equation 5.68, for different values of the SNR. The estimator in Equation 5.70 outperforms the other estimators for SNRs larger than 15 dB.

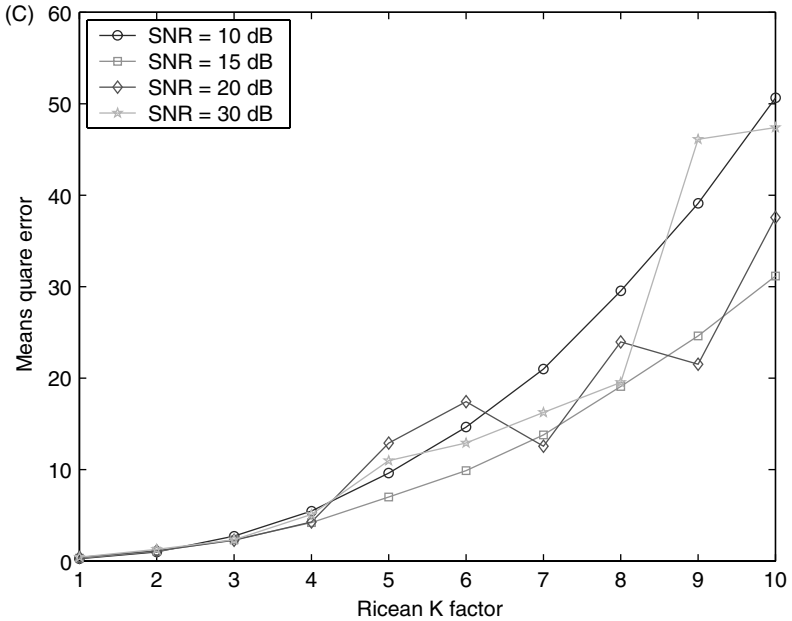

FIGURE 5.17 (*Continued*).

5.6.3 Simulation Results

In this section, the performance of the proposed estimators is compared to that of the COV-based estimator [24], [66]. The performance criterion is the mean square error of the estimators. The COV-based estimator is defined as [66]

$$\hat{K}_{COV} = \frac{\sigma_y^4 - c_{|y|^2}(0) + \sigma_y^2\sqrt{\sigma_y^4 - c_{|y|^2}(0)}}{c_{|y|^2}(0)} \tag{5.74}$$

where $c_{|y|^2}(\tau)$ refers to the covariance of $|y(t)|^2$ and σ_y^2 is the power of the received signal.

The mean square error (MSE) of the three estimators was computed over 1000 realizations of the received signal. Figure 5.17 shows the MSE of the estimators as a function of SNR. We observe that for SNRs larger than 15 dB, the estimator given by Equation 5.70 is superior to the estimators given by Equation 5.68 and Equation 5.74.

5.7 Application on Handover Performance

5.7.1 Handover Decision Algorithms

In cellular, microcellular, and picocellular systems, as a vehicule crosses the cell boundary between two BSs, control has to be transferred from the current BS to the target BS. This process is referred to as handover or handoff and is generally categorized into soft handoff and hard handoff processes [70, 75]. In hard handover processes, only one BS is in control of an MS at a given time. Soft handover processes require two or more BSs to be allocated to a single MS, in order to prevent the received signal power from dropping below a given threshold level. Soft handover processes are currently specific to CDMA systems where power control is critical [75]. The aim of this section is to study the effect of a biased velocity estimation

on the performance of handover decision algorithms. The derivations are done in the case of hard handoff processes but can also be adapted to soft handoff processes.

Consider an MS traveling from its current base station, BS1, to a target base station, BS2 (Figure 5.18). The decision to hand off is based on the received signal strength from both base stations. In the absence of shadowing, fading, and neglecting the effect of additive noise, the received signal envelopes are only affected by path loss. The path loss is inversely proportional to d^{α}, where d is the distance to the BS and α is a parameter determined by the environment. At mid-distance from the two BSs, the received strengths are identical, or equivalently, the difference between the two received strengths is zero. A decision to hand off from the current BS to the target BS could then be made when the sign of the difference between the two received strengths changes. However, in the presence of shadowing or fading, the sign can change several times around the cell boundary, which could result in a large number of unnecessary handovers. This is called the ping-pong effect. The effects of fast fading are significantly reduced through time-averaging the received signals over a window of size L. In [62], it was recommended that the window size corresponds to a distance of 40λ, hence to a period of time $T = 40\lambda/v$. Assuming the signal strengths are measured every T_s seconds, the time averaging should occur over $L = [\frac{40\lambda}{vT_s}]$ samples, where $[x] \leq x < [x] + 1$. The window size is therefore velocity dependent and is smaller for higher velocities than for smaller velocities.

5.7.2 Effect of an Error in Velocity Estimation on the System's Quality of Service

The quality of service of a system requires that the probability of a call being dropped must be less than p_{out}, where p_{out} is referred to as outage probability. Here we investigate how an error in velocity estimation δv would impact the probability of lost calls.

Every sampling time T_s, the MS of Figure 5.18 records measurements of the received signal strengths from BS1 and BS2 and computes a time average of the two received signal envelopes based on current and past measurements. Let $\Delta y_1(k)$ and $\Delta y_2(k)$ be the k^{th} sample of the time-averaged signals from BS1 and BS2, respectively. Assuming a measurement time $k \geq L$, $\Delta y_1(k)$ and $\Delta y_2(k)$ can be expressed as

$$\Delta y_i(k) = \frac{1}{L} \sum_{j=k-L+1}^{k} y_i(j), \quad i = \{1, 2\} \tag{5.75}$$

where $y_i(j)$ is the signal strength received from BSi at time j.

An error, δv, in velocity estimation leads to the choice of a temporal window

$$L' = \left[\frac{40\lambda}{(v + \delta v)T_s} \right] = L + \delta L \tag{5.76}$$

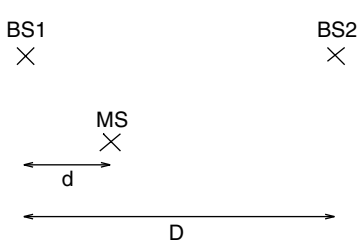

FIGURE 5.18 We consider an MS traveling from its current base station, BS1, toward a target base station, BS2.

where δL is a positive integer when δv is negative and a negative integer when δv is positive. It follows that the averaged signal strengths in Equation 5.75 become

$$\Delta' y_i(k) = \frac{1}{L+\delta L} \sum_{j=k-L-\delta L+1}^{k} y_i(j), \quad i = \{1,2\} \tag{5.77}$$

Assuming an error δL such that $\delta L / L \ll 1$, Equation 5.77 can be written as

$$\Delta' y_i(k) = \frac{1}{L}\left(1 - \frac{\delta L}{L}\right)\left[L\,\Delta y_i(k) + \sum_{j=k-L-\delta L+1}^{k-L} y_i(j)\right] \tag{5.78}$$

$$\delta L \geq 0 \tag{5.79}$$

$$\Delta' y_i(k) = \frac{1}{L}\left(1 - \frac{\delta L}{L}\right)\left[L\,\Delta y_i(k) - \sum_{j=k-L+1}^{k-L-\delta L} y_i(j)\right] \tag{5.80}$$

$$\delta L < 0 \tag{5.81}$$

where $\Delta y_i(k), i = \{1,2\}$, is defined in Equation 5.75. An error δL in window size leads to an error δe_i in average signal strength, where δe_i is defined as

$$\delta e_i(k) = \Delta' y_i(k) - \Delta y_i(k) \tag{5.82}$$

$$= \frac{1}{L} \sum_{k-L-\delta L+1}^{k-L} y_i(j) - \frac{\delta L}{L^2}\left[L\,\Delta y_i(k) + \sum_{k-L-\delta L+1}^{k-L} y_i(j)\right] \tag{5.83}$$

$$\delta L \geq 0 \tag{5.84}$$

$$\delta e_i(k) = -\frac{1}{L} \sum_{j=k-L+1}^{k-L-\delta L} y_i(j) - \frac{\delta L}{L^2}\left[L\,\Delta y_i(k) - \sum_{j=k-L+1}^{k-L-\delta L} y_i(j)\right] \tag{5.85}$$

$$\delta L < 0 \tag{5.86}$$

where $i = \{1,2\}$.

It is assumed, in handover decision algorithm design, that the process of time averaging has smoothed the effect of fast fading but not that of shadowing [51]. As a consequence, merely handing over from BS1 toward BS2 and back to BS1 when the difference $\Delta y_1(k) - \Delta y_2(k)$ changes sign would still result in a high number of unnecessary handovers. A more appropriate handover decision algorithm consists of handing over from BS1 toward BS2 when $\Delta y_1(k) - \Delta y_2(k) < -h$, and back to BS1 when $\Delta y_1(k) - \Delta y_2(k) > h$, where h is a hysteresis value determined by the system and by the environment (see Figure 5.19) [70]. The choice of h can be critical in terms of minimizing two conflicting criteria. If h is too small, shadowing is still dominant, resulting in a high number of unnecessary handovers. If h is too large, the handover process is delayed and a call could be lost.

A call is lost when the base station is BS1 and $\Delta y_1(k)$ drops below a given threshold th determined by the sensitivity of the receiver, or similarly, when the base station is BS2 and $\Delta y_2(k)$ is below th. The probability of a call being dropped at time k is then [70]

$$p_{LC}(k) = prob(BS1(k) \& \Delta y_1(k) < th) + prob(BS2(k) \& \Delta y_2(k) < th) \tag{5.87}$$

If an error δv occurs in the estimation of the velocity, a decision to hand off from BS1 toward BS2 would now be made when $\Delta' y_1(k) - \Delta' y_2(k) < -h$, and back to BS1 when $\Delta' y_1(k) - \Delta' y_2(k) > h$. Equivalently, a hand off toward BS2 would occur when $\Delta y_1(k) - \Delta y_2(k) < -h + \delta h$, and back to BS1 when $\Delta y_1(k) - \Delta y_2(k) > h + \delta h$, where $\delta h = \delta e_1(k) - \delta e_2(k)$. This could be interpreted as the decision to hand off in a system where the mobile velocity is known or is estimated in a very accurate way, but

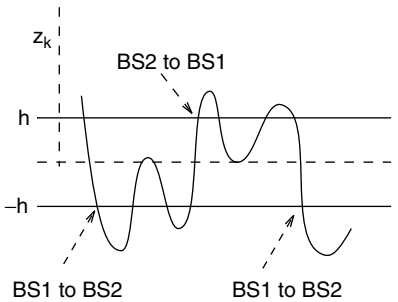

FIGURE 5.19 A handover is processed toward BS2 when $\Delta y_1(k) - \Delta y_2(k) < -h$, and back to BS1 when $\Delta y_1(k) - \Delta y_2(k) > h$, where h is a hysteresis value determined by the system and by the environment.

where two distinct hysteresis values, $h_1 = -h + \delta h$ and $h_2 = h + \delta h$, are used for handing over from BS1 to BS2 and from BS2 to BS1, respectively, where $h_1 \neq h_2$. It is assumed that the hysteresis value h was optimized so that the probability of lost calls resulting from a delay in handover is below the outage probability of the communications system. However, in the presence of an error in velocity estimation, if δh is negative, a delay in handing over from BS1 to BS2 occurs, and if δh is positive, a delay in handing over back to BS1 occurs. Either way, a delay in handover occurs, and depending on the value of δh, this delay could contribute to increasing the probability of losing a call. There is another way an error in velocity estimation can contribute to an increase in the probability of lost calls. Because of the error in velocity estimation, the probability of losing a call at time k is now

$$p_{LC}(k) = prob(BS1(k)\&\Delta y_1(k) < th - \delta e_1(k)) + prob(BS2(k)\&\Delta y_2(k) < th - \delta e_2(k)) \qquad (5.88)$$

Equation 5.88 can be interpreted as the probability of lost calls in a system where the mobile velocity is known or is estimated in a very accurate way, but where the sensitivity of the receiver is different. If $\delta e_1(k)$ and $\delta e_2(k)$ are positive, the receiver can be considered as having better sensitivity. However, if either $\delta e_1(k)$ or $\delta e_2(k)$ is negative, the sensitivity of the receiver could be considered worse, which could contribute to an increase in the probability of lost calls. In [29], it was found that an increase of 20% in velocity estimation error results in the probability of lost calls increasing by 50%.

5.8 Conclusions and Perspectives

This chapter outlined the principles and methods of velocity estimation, provided examples of velocity estimators, and gave a framework for analyzing the performance of velocity estimators. It also discussed the implications of erroneous velocity estimation on the wireless telecommunications systems and, more specifically, in the context of handover algorithm design. It was found that an error in velocity estimation could significantly deteriorate the quality of service of the system in terms of probability of dropped calls. The CDMA 2000 system is currently being implemented in Australia. Although the service provider, TELSTRA, sets the standards to be met by mobile phone manufacturers, it has no control over which or even if a velocity estimator is to be used by the telephone hand set manufacturer. As a result, two mobile phone sets from different manufacturers used at the same location can have different performances. This suggests the need, in the future, for more control over which standards are to be used by mobile phone manufacturers.

Acknowledgments

Prof. B. Boashash thanks the editor for his invitation to write this chapter. The material in the chapter is mostly extracted from the Ph.D. thesis of G. Azemi, whose supervisors were B. Boashash and B. Senadji. The authors also thank Dr. Sylvie Perreau and TELSTRA for technical discussions related to this chapter.

Appendix A: Derivation of Equation 5.39

In this appendix, we derive the first moment of the envelope of $|f_{i,s}|$. Using Equation 5.38, the expected value of $|f_{i,y}|$ can be written as

$$E\{|f_{i,y}|\} = \frac{1}{2\pi}\int_0^{\infty}\int_{-\pi}^{\pi}\int_{-\infty}^{\infty}\int_{-\infty}^{\infty} |\dot{\psi}|\; p(r,\psi,\dot{r},\dot{\psi})\; d\dot{\psi}\; d\dot{r}\; d\psi\; dr \tag{5.A1}$$

where $p(r,\psi,\dot{r},\dot{\psi})$ is the joint pdf of r, ψ, $\dot{r}$, $\dot{\psi}$. In the case of isotropic scattering, the joint pdf is given by [54]

$$\begin{aligned} p_1(r,\psi,\dot{r},\dot{\psi}) = {} & \frac{r^2}{4\pi^2 b_0 b_2} \\ & \times \exp\left(\frac{-1}{2b_0}(r^2 - 2Qr\cos\psi + Q^2)\right) \\ & \times \exp\left(\frac{-1}{2b_2}(\dot{r}^2 + r^2\dot{\psi}^2)\right) \end{aligned} \tag{5.A2}$$

Substituting Equation 5.A2 into Equation 5.A1, and since $p_1(r,\psi,\dot{r},\dot{\psi})$ is an even function of $\dot{\psi}$, Equation 5.A1 can now be written as

$$E\{|f_{i,y}|\} = \frac{1}{\pi}\int_0^{\infty}\int_{-\pi}^{\pi}\int_{-\infty}^{\infty}\int_{0}^{\infty} \dot{\psi}\; p_1(r,\psi,\dot{r},\dot{\psi})\; d\dot{\psi}\; d\dot{r}\; d\psi\; dr \tag{5.A3}$$

Using the following identities [23],

$$\int_{-\infty}^{\infty} \exp\left(\frac{-1}{2b_2}\dot{r}^2\right) d\dot{r} = \sqrt{2\pi b_2} \tag{5.A4a}$$

$$\int_0^{\infty} \dot{\psi}\; \exp\left(\frac{-1}{2b_2}r^2\dot{\psi}^2\right) d\dot{\psi} = b_2 r^{-2} \tag{5.A4b}$$

$$\int_{-\pi}^{\pi} \exp\left(\frac{1}{b_0}Qr\cos\psi\right) d\psi = 2\pi I_0\left(\frac{Q}{b_0}r\right) \tag{5.A4c}$$

$$\int_0^{\infty} \exp(-\mu^2x^2)\, I_0(\nu x)dx = \frac{\sqrt{\pi}}{2\mu}\exp\left(\frac{\nu^2}{8\mu^2}\right) I_0\left(\frac{\nu^2}{8\mu^2}\right) \tag{5.A4d}$$

in Equation 5.A3, we obtain

$$E\{|f_{i,y}|\} = \frac{1}{2\pi}\sqrt{\frac{b_2}{b_0}}\exp\left(\frac{-\rho}{2}\right) I_0\left(\frac{\rho}{2}\right) \tag{5.A5}$$

where $\rho = \frac{Q^2}{2b_0}$. In the absence of noise ($\gamma \to \infty$) and in the presence of isotropic scattering, b_0 and b_2 are equal to a_0 and $2\pi^2 f_m^2 a_0$, respectively, and since $K = \frac{\eta^2}{2\sigma^2}$, Equation 5.A5 becomes Equation 5.39.

Appendix B: Effect of the Scattering Distribution on the ZCR Method

In this appendix, we study the effect of nonisotropic scattering on the estimator in Equation 5.44, in the absence of shadowing and additive noise. In this case, ZCR_{x_i} in Equation 5.44 is given by Equation 5.32. From Equation 5.53, in the absence of shadowing and additive noise, b_0 and b_2 become M^2a_0 and M^2a_2,

respectively. In this case, Equation 5.44 reduces to

$$N_{\mathrm{ZCR}} = \frac{\nu}{\lambda}\sqrt{q_2(\chi)} \tag{5.B1}$$

It follows that the normalized bias for the ZCR-based velocity estimator is derived as

$$\varepsilon(\chi, \infty, K) = \sqrt{2q_2(\chi)} - 1 \tag{5.B2}$$

which is the same as Equation 5.57. Equation 5.B2 proves that both ZCR and IF-based estimators have the same performances in the presence of nonisotropic scattering.

Appendix C: SNR Improvement in the IF Estimator

In this appendix, we prove that the IF estimator improves the SNR. If we assume that the power of the noise at the input of the IF estimator is $N_0 B_0$, the SNR at the input of the IF estimator is derived as

$$\gamma_R = \left(\frac{S}{N}\right)_R = \frac{A^2}{2N_0 B_0} \tag{5.C1}$$

Based on the results in [18, Section 10.3], when γ_R is more than a threshold level[3], the signal $y_{out}(t)$ at the output of the IF estimator, can be expressed as

$$y_{out}(t) = f_{i,y}(t) = f_{i,s}(t) + \xi(t)$$

where $\xi(t)$ represents the IF noise. The PSD of the IF noise is given by [18, p. 414]

$$S_\xi(f) = \frac{N_0 f^2}{A^2} \prod\left(\frac{f}{B_0}\right)$$

where $\prod(\,.\,)$ represents the rectangular pulse function. Thus, the power of the IF noise in the frequency band $(f_1, \frac{B_0}{2})$ can then be computed as

$$N_D = 2\int_{f_1}^{\frac{B_0}{2}} S_\xi(f)df = \frac{2N_0}{3A^2}\left(\frac{B_0^3}{8} - f_1^3\right)$$

The power of $f_i(t)$ in the frequency band $(f_1, \frac{B_0}{2})$ can also be computed as [43, p. 256]

$$S_D = \left(\frac{1}{4\pi^2}\right) 2\int_{f_1}^{\frac{B_0}{2}} S_\phi(f)df = \frac{B_0^2}{8}\ln\frac{B_0}{2f_1}$$

Therefore, assuming $f_1 \ll B_0$, the SNR at the output of the IF estimator can be derived as

$$\gamma_D = \left(\frac{S}{N}\right)_D \simeq 3\gamma_R \ln\frac{B_0}{2f_1} \tag{5.C2}$$

It follows from Equation 5.C2 that the IF estimator improves the SNR by a factor $3\ln\frac{B_0}{2f_1}$.

[3]This threshold is found to occur in the vicinity of 10-dB input SNR and varies in the approximate range of 6 to 13 dB [67, p. 458].

References

[1] A. Abdi and M. Kaveh. A new velocity estimator for cellular systems based on higher order crossings. In *Proceeding of the Asilomar Conference on Signals, Systems, and Computers*, Vol. 2, 1998, pp. 1423–1427.

[2] M.G. Amin. Interference mitigation in spread spectrum communication systems using time-frequency distributions. *IEEE Trans. Signal Process.*, 45, Jan. 1997.

[3] M.G. Amin, C. Wang, and A.R. Lindsey. Optimum interference excision in spread spectrum communications using open-loop adaptive filters. *IEEE Trans. Signal Process.*, 47,1966–1976, 1999.

[4] M. Anderson and S. Perreau. Robust power control for cdma networks subject to modelisation errors. In *Proceedings of the IEEE International Conference on Acoustics, Speech, and Signal Processing, ICASSP'03*, Hong Kong, 2003, pp. 612–619.

[5] K.D. Anim-Appiah. On generalized covariance-based velocity estimation. *IEEE Trans. Veh. Technol.*, 48, 1546–1557, 1999.

[6] M.D. Austin and G.L. Stüber. Eigen-based doppler estimation for differentially coherent CPM. *IEEE Trans. Veh. Technol.*, 43, 781–785, 1994.

[7] M.D. Austin and G.L. Stüber. Velocity adaptive handoff algorithms for microcellular systems. *IEEE Trans. Veh. Technol.*, 43, 549–561, 1994.

[8] G. Azemi. Mobile Velocity Estimation Using a Time-Frequency Approach. Ph.D. thesis, Queensland University of Technology, Brisbane, Australia, 2003.

[9] G. Azemi, B. Senadji, and B. Boashash. Mobile unit velocity estimation based on the instantaneous frequency of the received signal. Submitted.

[10] G. Azemi, B. Senadji, and B. Boashash. Mobile unit velocity estimation in micro-cellular systems using the ZCR of the instantaneous frequency of the received signal. In *Proceedings of the International Symposium on Signal Processing and Its Applications, ISSPA'03*, Vol. 2, Paris, France, 2003, pp. 289–292.

[11] G. Azemi, B. Senadji, and B. Boashash. A novel estimator for the velocity of a mobile station in a microcellular system. In *Proceedings of the International Symposium on Circuits and Systems, ISCAS'03*, Vol. 2, Bangkok, Thailand, May 2003, pp. 212–215.

[12] S. Barbarossa and A. Scaglione. Optimal precoding for transmissions over linear time-varying channels. In *Seamless Interconnection for Universal Services, GLOBECOM'99*, Vol. 5, Piscataway, NJ, 1999, pp. 2545–2549.

[13] A. Belouchrani and M.G. Amin. Blind source separation based on time–frequency signal representations. *IEEE Trans. Signal Process.*, 46, 2888–2897, 1998.

[14] B. Boashash. Estimating and interpreting the instantaneous frequency of a signal. Part 1. Fundamentals. *Proc. IEEE*, 80, 519–538, 1992.

[15] B. Boashash. Estimating and interpreting the instantaneous frequency of a signal. Part 2. Algorithms and applications. *Proc. IEEE*, 80, 539–568, 1992.

[16] B. Boashash, Ed. *Time-Frequency Signal Analysis and Processing: A Comprehensive Reference*. Elsevier, Amsterdam, 2003.

[17] B. Boashash, A. Belouchrani, K. Abed-Meraim, and L.-T. Nguyen. Time-frequency signal processing for wireless communications. Chapter 25 in *Signal Processing for Mobile Communications Handbook*, CRC Press, Boca Raton, FL, M. Ibnkahla, Ed. 2003.

[18] A.B. Carlson, P.B. Crilly, and J.C. Rutledge. *Communication Systems: An Introduction to Signals and Noise in Electrical Communication*, 4th ed. McGraw-Hill, New York, 2002.

[19] A. Chockalingam, P. Dietrich, L.B. Milstein, and R.R. Rao. Performance of closed-loop power control in DS-CDMA cellular systems. *IEEE Trans. Veh. Technol.*, 47, 774–789, 1998.

[20] M.J. Chu and W.E. Stark. Effect of mobile velocity on communications in fading channels. *IEEE Trans. Veh. Technol.*, 49, 202–210, 2000.

[21] Standard Document, Ed. *Physical Layer Standard for CDMA 2000 Spread Spectrum Systems*. 3GPP, 1999.

[22] H.S.H. Gombachika and O.K. Tonguz. Influence of multipath fading and mobile unit velocity on the performance of PN tracking in CDMA systems. In *Proceedings of the Vehicular Technology Conference, IEEE 47th*, Vol. 3, 1997, pp. 2206–2209,
[23] I.S. Gradshteyn and I.M. Ryzhik. *Table of Integrals, Series, and Products*. Academic Press, New York, 1994.
[24] D.G. Greenstein, L.J. Michelson, and V. Erceg. Moment-method estimation of the Ricean K-factor. *IEEE Commun. Lett.*, 3, 175–176, 1999.
[25] D. Greenwood and L. Hanzo. Characterization of mobile radio channels. In *Mobile Radio Communications,* R. Steele, Ed., Pentech, London, 1992, pp. 163–185.
[26] H. Hansen, S. Affes, and P. Mermelstein. A Rayleigh Doppler frequency estimator derived from maximum likelihood theory. In *IEEE Workshop on Signal Processing Advances in Wireless Communications, SPAWC'99*, 1999, pp. 382–386.
[27] R. Hass and J.C. Belfiore. A time–frequency well-localized pulse for multiple carrier transmission. *Wireless Personal Commun.*, 5, 1–18, 1997.
[28] M. Hellebrandt, R. Mathar, and M. Scheibenbogen. Estimating position and velocity of mobiles in a cellular radio network. *IEEE Trans. Veh. Technol.*, 46, 65–71, 1997.
[29] E. Holmbakken, G. Azemi, V. Karawalevu, and B. Senadji. The importance of accurate velocity estimation in designing handover algorithms for microcellular systems. In *Workshop on Signal Processing and Applications, WoSPA*, Brisbane, Australia, December 2002.
[30] J.M. Holtzman. Adaptive measurement intervals for handoffs. In *Proceedings of the IEEE International Conference on Communications, ICC*, Vol. 2, June 1992, pp. 1032–1036.
[31] J.M. Holtzman and A. Sampath. Adaptive averaging methodology for handoffs in cellular systems. *IEEE Trans. Veh. Technol.*, 44, 59–66, 1995.
[32] M. Ibnkahla, Ed. *Signal Processing for Mobile Communications Handbook*. CRC Press, Boca Raton FL, 2003.
[33] K. Ivanov and G. Spring. Mobile speed sensitive handover in a mixed cell environment. In *Proceedings of the Vehicular Technology Conference, IEEE 45th*, Vol. 2, 1995, pp. 892–896.
[34] W.C. Jakes, Ed. *Microwave Mobile Communication*. IEEE Press, Washington, DC, 1974.
[35] Z.M. Kamran, A.R. Leyman, and K. Abed-Meraim. Techniques for blind source separation using higher-order statistic. In *IEEE Workshop on Statistical Signal and Array Processing, Pennsylvania, USA*, August 2000, pp. 334–338.
[36] K. Kawabata, T. Nakamura, and E. Fukuda. Estimating velocity using diversity reception. In *Proceedings of the Vehicular Technology Conference, IEEE 44th*, Vol. 1, 1994, pp. 371–374.
[37] T. Keller and L. Hanzo. Adaptive multicarrier modulation: a convenient framework for time-frequency processing in wireless communications. *Proc. IEEE*, 88, 611–640, 2000.
[38] J.E. Kleider and M.E. Humphrey. Robust time-frequency synchronization for OFDM mobile applications. In *Proceedings of the International Symposium on Signal Processing and Its Applications, ISSPA'99*, Vol. 1, 1999, pp. 423–426.
[39] Y.C. Ko and G. Jeong. Doppler spread estimation in mobile communication systems. In *Proceedings of the Vehicular Technology Conference, IEEE 55th*, Vol. 4, 2002, pp. 1941–1945.
[40] L. Krasny, H. Arslan, D. Koilpillai, and S. Chennakeshu. Doppler spread estimation in mobile radio systems. *IEEE Commun. Lett.*, 5, 197–199, 2001.
[41] A. Kurniawan, S. Perreau, J. Choi, and K. Lever. Power control and diversity antenna arrays for cdma systems. In *Proceedings of the International Conference on Information, Communications and Signal Processing*, Singapore, 2001.
[42] H. Lee and D. Cho. A new adaptive power control scheme based on mobile velocity in wireless mobile communication systems. In *Proceedings of the Vehicular Technology Conference, IEEE 53rd*, Vol. 4, 2001, pp. 2878–2882.
[43] W.C.Y. Lee. *Mobile Communication Engineering: Theory and Applications*. McGraw-Hill, New York, 1998.

[44] W.C.Y. Lee and Y.S. Yeh. On the estimation of the second-order statistics of log-normal fading in mobile radio environment. *IEEE Trans. Commun.*, 22, 809–873, 1974.
[45] J. Lin and J.G. Proakis. A parametric method for Doppler spectrum estimation in mobile radio channels. In *27th Conference on Information Systems and Sciences*, March 1993, pp. 875–880.
[46] T.L. Marzetta. EM algorithm for estimating the parameters of a multivariate complex Rician density for polarimetric SAR. In *Proceedings of the IEEE International Conference on Acoustics, Speech, and Signal Processing, ICASSP'95*, Vol. 5, May 1995, pp. 3651–3654.
[47] P.E. Mogensen, P. Eggers, C. Jensen, and J.B. Andersen. Urban area radio propagation measurements at 995 and 1845 MHz for small and micro-cells. In *Proceedings of the Global Communication Conference*, Vol. 2, December 1991, pp. 1297–1302.
[48] D. Mottier and D. Castelain. A Doppler estimation for UMTS-FDD based on channel power statistics. In *Proceedings of the Vehicular Technology Conference, IEEE 50th*, Vol. 5, Fall 1999, pp. 3052–3056.
[49] R. Narasimhan and D.C. Cox. Speed estimation in wireless systems using wavelets. *IEEE Trans. Commun.*, 47, 1357–1364, 1999.
[50] R. Narasimhan and D.C. Cox. Estimation of mobile speed and average received power in wireless systems using best basis methods. *IEEE Trans. Commun.*, 49, 2172–2183, 2001.
[51] G.P. Pollini. Trends in handover design. *IEEE Commun. Mag.*, 34, 82–89, 1996.
[52] J.G. Proakis. *Digital Communications*, 3rd ed. McGraw-Hill, New York, 1995.
[53] S.O. Rice. Mathematical analysis of random noise. *Bell System Tech. J.*, 24, 46–156, 1945.
[54] S.O. Rice. Statistical properties of a sine wave plus random noise. *Bell System Tech. J.*, 109–157, 1948.
[55] A. Sampath and J.M. Holtzman. Estimation of maximum Doppler frequency for handoff decisions. In *Proceedings of the Vehicular Technology Conference, IEEE 43rd*, 1993, pp. 859–862.
[56] A.M. Sayeed. Canonical time-frequency processing for broadband signaling over dispersive channels. In *Proceedings of the IEEE-SP International Symposium on Time-Frequency and Time-Scale Analysis*, New York, 1998, pp. 369–372.
[57] A.M. Sayeed and B. Aazhang. Communication over multipath fading channels: a time-frequency perspective. Chapter 3 in *Wireless Communications: TDMA versus CDMA*, S.G. Glisic and P.A. Leppanen, Eds. Kluwer Academic, Dordrecht, Netherlands, 1997.
[58] A.M. Sayeed and B. Aazhang. Joint multipath-Doppler diversity in mobile wireless communications. *IEEE Trans. Commun.*, 47, 123–132, 1999.
[59] A.M. Sayeed, A. Sendonaris, and B. Aazhang. Multiuser detection in fast-fading multipath environments. *IEEE J. Selected Areas Commun.*, 16, 1691–1701, 1998.
[60] A. Scaglione, S. Barbarossa, and G.B. Giannakis. Optimal adaptive precoding for frequency-selective Nakagami-m fading channels. In *Proceedings of the Vehicular Technology Conference, IEEE 52nd*, Vol. 3, 2000, pp. 1291–1295.
[61] W. Sheng and S.D. Blostein. SNR-independent velocity estimation for mobile cellular communications systems. In *Proceedings of the IEEE International Conference on Acoustics, Speech, and Signal Processing, ICASSP'02*, Vol. 3, 2002, pp. 2469–2472.
[62] G.L. Stüber. *Principles of Mobile Communication*. Kluwer Academic Publishers, Dordrecht, Netherlands, 1996.
[63] K.K. Talukdar and W.D. Lawing. Estimation of the parameters of the Rice distribution. *J. Acoust. Soc. Am.*, 89, 1193–1197, 1991.
[64] C. Tepedelenlioğlu, A. Abdi, and G.B. Giannakis. The Ricean K factor: estimation and performance analysis. 2, 799–810, 2003.
[65] C. Tepedelenlioğlu, A. Abdi, G.B. Giannakis, and M. Kaveh. Review: estimation of Doppler spread and signal strength in mobile communications with applications to handoff and adaptive transmission. *Wireless Commun. Mobile Comput.*, 1, 221–242, 2001.
[66] C. Tepedelenlioğlu and G.B. Giannakis. On velocity estimation and correlation properties of narrowband mobile communication channels. *IEEE Trans. Veh. Technol.*, 50, 1039–1052, 2001.

[67] J.B. Thomas. *An Introduction to Statistical Communication Theory*. John Wiley & Sons, New York, 1967.

[68] M. Türkboylari and G.L. Stüber. Eigen-matrix pencil method-based velocity estimation for mobile cellular radio systems. In *Proceedings of the IEEE International Conference on Communications, ICC*, Vol. 2, 2000, pp. 690–694.

[69] R. Vijayan and J.M. Holtzman. Analysis of handoff algorithms using nonstationary signal strength measurements. In *Proceedings of the IEEE Global Telecommunications Conference, GLOBCOM'92*, Vol. 3, December 1992, pp. 1405–1409.

[70] R. Vijayan and J.M. Holtzman. A model for analyzing handoff algorithms (cellular radio). *IEEE Trans. Veh. Technol.*, 42, 351–356, 1993.

[71] L. Wang, M. Silventoinen, and Z. Honkasalo. A new algorithm for estimating mobile speed at the TDMA-based cellular system. In *Proceedings of the Vehicular Technology Conference, IEEE 46th*, Vol. 2, 1996, pp. 1145–1149.

[72] Y. Wang, L. Gao, M. Zhao, J. Chen, Z. Zhang, and Y. Yao. Time-frequency code for multicarrier DS-CDMA systems. In *Proceedings of the Vehicular Technology Conference, IEEE 55th*, Vol. 3, 2002, pp. 1224–1227.

[73] C. Xiao. Estimating velocity of mobiles in EDGE systems. In *Proceedings of the IEEE International Conference on Communications, ICC*, Vol. 5, 2002, pp. 3240–3244.

[74] C. Xiao, K.D. Mann, and J.C. Oliver. Mobile speed estimation for TDMA-based hierarchical cellular systems. *IEEE Trans. Veh. Technol.*, 50, 981–991, 2001.

[75] N. Zhang and J.M. Holtzman. Analysis of cdma soft-handoff algorithm. *IEEE Trans. Veh. Technol.*, 47, 710–718, 1998.